International Journal of Greenhouse Gas Control 147 (2025) 104478

Contents lists available at ScienceDirect

International Journal of Greenhouse Gas Control

journal homepage: www.elsevier.com/locate/ijggc

Integration of CASOH and DISPLACE technologies in a steel plant for the mitigation of CO_2 emissions – A techno-economic analysis

Nicola Zecca [a,*], Santiago Zapata Boada [b], Vincenzo Spallina [b], Giampaolo Manzolini [a]

[a] Politecnico di Milano, Dipartimento di Energia, via Lambruschini 4, 20126, Milano, Italy
[b] Department of Chemical Engineering, University of Manchester, Manchester M13 9PL, UK

ARTICLE INFO

Keywords:
CASOH
DISPLACE
Steel
CCS
Techno-economic analysis

ABSTRACT

Given the severe climate crisis and the urgent need to limit the adverse effects of global warming, drastic changes are required across various industries. Among them, the iron and steel sector is a major contributor to greenhouse gas emissions, accounting for approximately 7 % of global CO_2 emissions. This study proposes the integration of innovative carbon capture technologies, such as DISPLACE and CASOH, into a conventional BF-BOF (Blast Furnace-Basic Oxygen Furnace) steelmaking process. A comprehensive techno-economic analysis was conducted, supported by simulations performed in Aspen Plus, to optimize the integration of these technologies. The study suggests a redesigned gas distribution system within the BF-BOF steel plant, incorporating oxy-fired units to facilitate post-combustion carbon capture and minimize the plant emissions. The analysis reveals that, employing CASOH for pre-combustion CO_2 capture to decarbonize a mixture of BFG (Blast Furnace Gas) and BOFG (Basic Oxygen Furnace Gas), combined with DISPLACE for decarbonizing flue gases from hot stoves, sinter plant, and reheating ovens, 72 % reduction in CO_2 emissions and a SPECCA around 0 GJ/t_{CO2} can be achieved. This is attainable within a renewable electricity scenario, at a cost of 138 € per ton of CO_2 avoided. Lower CO_2 avoidance values can also be achieved by treating less exhaust gases with reduction in both SPECCA and costs.

1. Introduction

The iron and steel industry which account for about 7 % of global direct energy-related CO_2 emissions faces significant challenges in reducing emissions due to its heavy reliance on fossil fuels, particularly coal, in the blast furnace-basic oxygen furnace (BF-BOF) steelmaking route, which currently dominates the steel market, accounting for 70 % of global steel production and 90 % of primary production (International Energy Agency, 2020). Another primary production method is the direct reduced iron-electric arc furnace (DRI-EAF) route, which differs from BF-BOF by using high-quality DRI pellets instead of raw iron ore. Reduction occurs in a solid state in the DRI furnace before melting in the EAF, often combined with scrap. This route utilizes hydrogen and carbon monoxide as reducing agents, with natural gas predominantly used to generate the required syngas (International Energy Agency, 2020). Secondary steel production which represents approximately 22 % of total steel production, primarily relies on electricity to melt scrap in electric arc furnaces which operate at high temperatures facilitated by conductive graphite electrodes (International Energy Agency, 2020).

Integrating carbon capture technologies into steel production processes is essential for progressing towards a net-zero emissions future. Perpiñán et al. (2023) conducted a systematic review of peer-reviewed articles focused on the integration of carbon capture technologies in the BF-BOF steelmaking route, categorizing the carbon capture technologies into four main groups: i) post-combustion (chemical absorption, membranes), ii) looping processes (calcium looping, chemical looping, other looping processes), iii) oxygen blast furnaces and top-gas recycling, and iv) pre-combustion (chemical absorption, adsorption, membranes, SEWGS). These technologies are compared considering 6 KPIs: thermal penalty (GJ/t_{CO2}), electrical penalty (GJ/t_{CO2}), economic cost (\$/t_{CO2}), CO_2 emission reduction, (kg/t_{HM}), CO_2 purity (%) and TRL as reported in Table 1.

Chemical absorption has been extensively investigated for post-combustion CO_2 capture from flue gases of hot stoves (Chamchan et al., 2017; Cheng et al., 2010; Goto et al., 2011), of power plant (Gazzani et al., 2015; Manzolini et al., 2020; Sundqvist et al., 2018), and of coke ovens (Oko et al., 2018; Wiley et al., 2011). To enhance CO_2 emission reductions, concurrent carbon capture from multiple sources has been studied (Arasto et al., 2013b; Yun et al., 2021). The most commonly evaluated amines are monoethanolamine (MEA) and methyldiethanolamine (MDEA) with other solvents seldomly addressed in

* Corresponding author.
E-mail address: nicola.zecca@polimi.it (N. Zecca).

https://doi.org/10.1016/j.ijggc.2025.104478
Received 11 February 2025; Received in revised form 31 July 2025; Accepted 14 September 2025
Available online 30 September 2025

Nomenclature

Acronyms

ASU	Air Separation Unit
BF	Blast Furnace
BFG	Blast Furnace Gas
BOF	Basic Oxygen Furnace
BOFG	Basic Oxygen Furnace Gas
CCA	Cost of CO_2 Avoided [€/t_{CO2}]
CCR	Carbon Capture Ratio [%]
COG	Coke Oven Gas
CP	Carbon Purity [%]
DRI	Direct Reduced Iron
EAF	Electric Arc Furnace
FCF	Fixed Charge Factor
HM	Hot Metal
HS	Hot Stoves
KPI	Key Performance Indicators
LCOH	Levelized Cost of Hydrogen [€/kg_{H2}]
LCOHRC	Levelized Cost of Hot Rolled Coil [€/t_{HRC}]
MDEA	Methyldiethanolamine
MEA	Monoethanolamine
MP	Medium Pressure
MPS	Medium Pressure Steam
MPW	Medium Pressure Water
NG	Natural Gas
NGCC	Natural Gas Combined Cycle
OBF	Oxy Blast Furnace
PEC	Primary Energy Consumption [GJ/t_{HRC}]
RES	Renewable Energy Sources
RO	Reheating Ovens
SEWGS	Sorption Enhanced Water Gas Shift
SP	Sinter Plant
SPECCA	Specific PEC per unit of CO_2 Avoided [GJ/t_{CO2}]
TAC	Total Annualised Cost [M€/y]
TEC	Total Equipment Cost [€]
TGR	Top Gas Recycling
TPC	Total Plant Cost [€]
TRL	Technology Readiness Level
WGS	Water Gas Shift

Symbols

e_{CO2}	Specific CO_2 emissions [$t_{CO2}/t_{product}$]
h_{eq}	Equivalent hours [h/y]
$\dot{m}$	Mass flowrate [kg/s]
p	Pressure [bar]
Δp	Pressure drops [bar]
T	Temperature [°C]
ΔT	Temperature difference [°C]

Subscripts

h	Hydraulic
is	Isentropic
m	Mechanical
p	Polytropic
th	Thermal

Greek

η	Efficiency [-]

literature. Relatively few theoretical studies regarding the use of membranes in post-combustion mode are present in literature, due to the still low TRL of membranes in the iron and steel industry (Baker et al., 2018; Luca and Petrescu, 2021; Yun et al., 2021). However, membranes can achieve high CO_2 purity levels.

In the case of calcium looping, many studies consider the decarbonisation of various CO_2 sources, such as blast furnace gas (BFG), basic oxygen furnace gas (BOFG), coke oven gas (COG), or flue gas from hot stoves or lime kilns (Chisalita et al., 2019; Cormos et al., 2020a; Hallmann and Steinfeld, 2015; Tian et al., 2018). Some studies have focused on applying the chemical looping concept for the combustion of coke oven gases (COG) without CO_2 emissions or for producing hydrogen for the steelmaking process (Katayama et al., 2020; Luo et al., 2018; Xiang and Zhao, 2018). Similarly, other looping processes have been evaluated for the decarbonization of BFG, BOFG, and COG (Fernández et al., 2020, 2017; Martínez et al., 2019, 2018a; Sun et al., 2020). Nevertheless, in both cases, the TRL is still low.

Oxygen blast furnaces (OBF) and top-gas recycling (TGR) strategies are among the most widely investigated methods in the iron and steel industry for mitigating CO_2 emissions. These concepts were optimised and tested in the context of the ULCOS project (Arasto et al., 2014; Ho et al., 2013; Jin et al., 2016; Li et al., 2020; Qie et al., 2020; She et al., 2017; Tsupari et al., 2015; Zuo Guangqing and Hirsch A., 2009). In OBF, oxygen-enriched hot-blast air is used in the shaft furnace for coke combustion, resulting in a more CO_2-concentrated blast furnace top gas due to the reduced nitrogen content. The TGR concept involves recycling a portion of the top gas back to the blast furnace, after a CO_2 capture stage.

Chemical absorption technology is also studied in the steel industry for pre-combustion carbon capture configuration (Birat, 2010; Gazzani et al., 2015; Martinez Castilla et al., 2019; Sundqvist et al., 2018). MEA, MDEA and piperazine are the most investigated solvents. In the case of adsorption, the vacuum-pressure swing adsorption process is the most investigated and is usually coupled with the TGR concept, processing blast furnace gas (Abdul Quader et al., 2016; Danloy et al., 2009; Jin et al., 2017; Kim et al., 2015; Quader et al., 2016; Sahu et al., 2015; She et al., 2017). Membranes can also be used in pre-combustion mode (Chung et al., 2018a; Jeon et al., 2022; Li et al., 2022; Ramírez-Santos et al., 2018). According to Hasan et al. 2012, membrane separation is preferable to amine scrubbing for CO_2 concentrations above 36 %. Most studies focus on the decarbonization of BFG, demonstrating low costs but also indicating a low TRL. Finally, the use of Sorption-Enhanced Water-Gas Shift (SEWGS) has been investigated for the pre-combustion decarbonization of gases typically used as fuel in the power plants of BF-BOF steel mills (Gazzani et al., 2015; Manzolini et al., 2020; Petrescu et al., 2019; van Dijk et al., 2018).

In general, the thermal penalty for various carbon capture technologies varies between 1.3 and 6.2 GJ/t_{CO2} (Perpiñán et al., 2023). When it comes to electricity consumption, post-combustion chemical absorption, calcium looping, and pre-combustion chemical absorption generally have lower electricity requirements, averaging less than 1 GJ/t_{CO2} because heat consumption is predominant, with most of electricity usage related to CO_2 compression (Perpiñán et al., 2023). On the other hand, technologies like membranes (post- and pre-combustion), and adsorption pre-combustion requires a compression step upstream the CO_2 capture process, leading to higher electricity penalties between 1 and 3 GJ/t_{CO2} (Perpiñán et al., 2023). It must be noted that low energy penalties and low costs are typically associated to low TRL concepts, while higher penalties and costs are related to high TRL technologies.

1.1. The DISPLACE technology

The DISPLACE technology (Downstream Integrated Steel Production with Advanced CO_2 Capture) is a multicolumn post-combustion CO_2

Table 1
Main KPIs for carbon capture technologies integrated in steel plants. Adapted from Perpiñán et al. (2023).

CC technology	CO_2 source	Thermal penalty [GJ/t_{CO2}]	Electrical penalty [GJ/t_{CO2}]	Cost [$/$t_{CO2}$]	Emissions reduction [t_{CO2}/t_{steel}]	CO_2 purity [%]	TRL	References
Post combustion								
- Chemical absorption	Hot stoves, power plant, coke ovens, lime kilns, sinter plant	2.3 – 6.5	0.28 – 1.5	38 – 204	0.2 – 1.7	> 95	2 – 5	(Arasto et al., 2013a, 2013b; Biermann et al., 2019; Chamchan et al., 2017; Cheng et al., 2010; Chisalita et al., 2019; Cormos et al., 2020a; Cormos, 2016; Gazzani et al., 2015; Goto et al., 2011; Ho et al., 2011; Manzolini et al., 2020; Martínez et al., 2018b; Oko et al., 2018; Sundqvist et al., 2018; Tsupari et al., 2013; Wiley et al., 2011; Yun et al., 2021)
- Membrane	Hot stoves, power plant, coke ovens, lime kilns, sinter plant	n/a	0.9 – 4.4	36 – 252.7	n/a	> 90	3 – 6	(Baker et al., 2018; Luca and Petrescu, 2021; Yun et al., 2021)
Looping processes								
- Calcium looping	BFG, BOFG, COG, hot stoves, lime kilns	2.7 – 5.6	0.1 – 2.5	60.2 – 73.8	1 – 1.7	> 95	2 – 3	(Chisalita et al., 2019; Cormos et al., 2020a; Cormos, 2016; Halmann and Steinfeld, 2015; Tian et al., 2018; Xie et al., 2017)
- Chemical looping	COG, sinter plant	n/a	n/a	n/a	n/a	90	2 – 4	(Katayama et al., 2020; Luo et al., 2018; Xiang and Zhao, 2018)
- Other processes	BFG, BOFG, COG	1.4 – 4.3	n/a	n/a	0.5 – 1.6	57 – 99.9	3 – 5	(Fernández et al., 2020, 2017; Martínez et al., 2019, 2018a; Sun et al., 2020)
TGR-OBF	BFG	0.3	1.4 – 5.6	50 – 90	0.1 – 0.6	n/a	2 – 6	(Arasto et al., 2014; Ho et al., 2013; Jin et al., 2016; Li et al., 2020; Qie et al., 2020; She et al., 2017; Tsupari et al., 2015; Zuo Guangqing and Hirsch A., 2009)
Pre-combustion								
- Chemical absorption	BFG, BOFG, COG	1.3 – 4.4	0.2 –1.2	40.6 – 97	0.6 – 1	> 90	2 – 6	(Birat, 2010; Chung et al., 2018b; Gazzani et al., 2015; Ho et al., 2011; Martinez Castilla et al., 2019; Onarheim and Arasto, 2016; Sundqvist et al., 2018)
- Adsorption	BFG, OBFG	n/a	0.4 – 2.7	60	0.5 – 1.2	> 79.9	2 – 6	(Abdul Quader et al., 2016; Danloy G. et al., 2009; Ho et al., 2013; Jin et al., 2017; Kim et al., 2015; Quader et al., 2016; Sahu et al., 2015; She et al., 2017)
- Membranes	BFG, BOFG	n/a	0.4 – 1.6	28.8 – 50.6	0.8	> 55	2 – 4	(Chung et al., 2018a; Jeon et al., 2022; Li et al., 2022; Ramírez-Santos et al., 2018)
- SEWGS	BFG, BOFG, COG	n/a	1.9 – 2.9	36.4	0.6 – 0.8	> 96.8	2 – 6	(Gazzani et al., 2015; Manzolini et al., 2020; Petrescu et al., 2019; van Dijk et al., 2018)

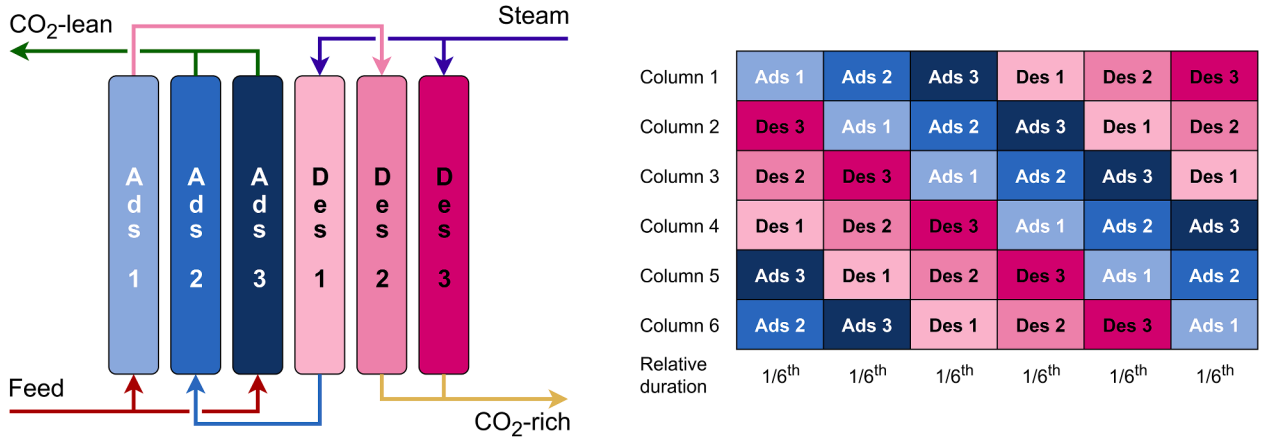

Fig. 1. Six column DISPLACE process (left) and timing for a 6-column unit (right). The column names indicate which product gas they are producing. Adapted from Zecca et al. (2025).

capture system. It operates on an isobaric concentration swing principle, delivering two separate product streams at unit operating pressure (Fig. 1). In the feed step, CO_2 is adsorbed onto a sorbent, generating a CO_2-lean stream, while the sorbent is regenerated by displacing CO_2 with steam, resulting in a CO_2-rich product, without requiring pressure or temperature swings. In the process, the CO_2 is adsorbed onto the sorbent due to its high partial pressure. The sorbent commonly used is K-promoted hydrotalcite. To achieve a continuous process, the DISPLACE cycle development is based on the following constraints: i) one column always receives feed; ii) one column always produces the CO_2-lean product; iii) one column always produces the CO_2-rich product; iv) steam consumption is reduced by recycling Ads-1 within the cycle; v) CO_2 purity is increased by recycling Des-1 within the cycle. Compared to SEWGS, although the DISPLACE process operates at a lower pressure, it generates a CO_2-rich product at higher pressure. The CO_2 concentration in the CO_2-rich stream is regulated by adjusting the amount of steam fed to the DISPLACE unit, as well as through the recycling of the Des-1 stream. Additionally, to prevent the build-up of impurities within the

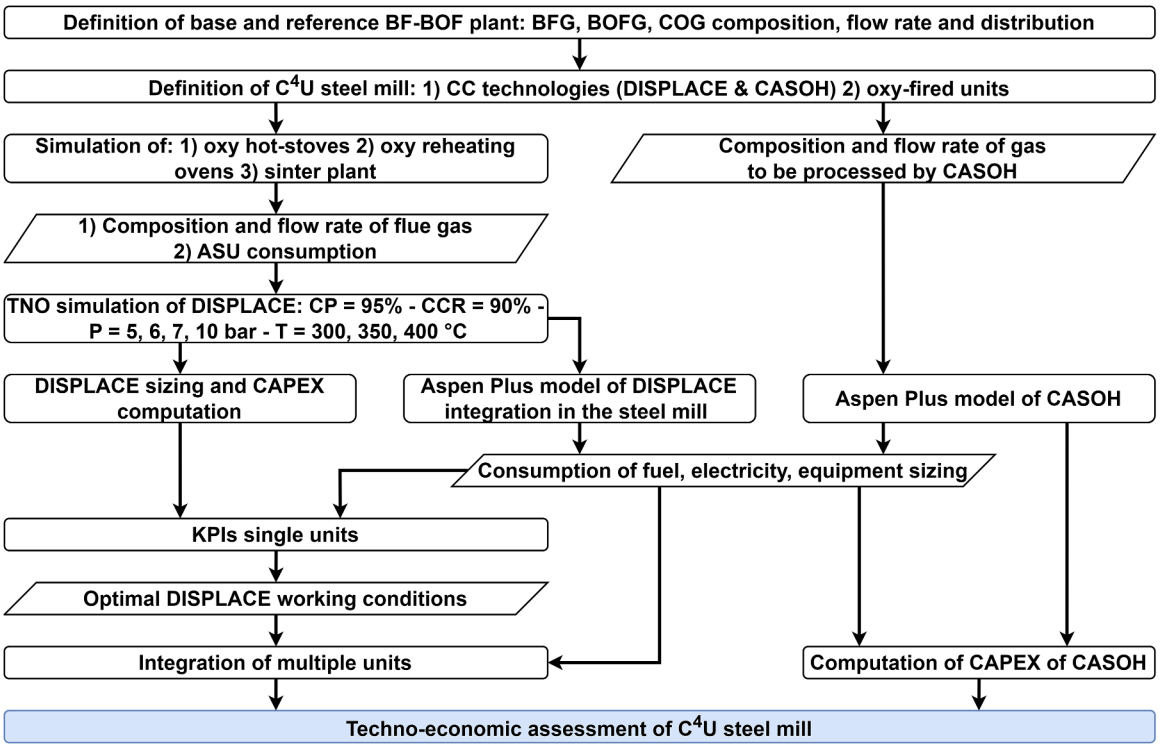

Fig. 2. Methodology adopted for the techno-economic assessment of the C^{4}U steel mill.

system, a flushing step is implemented in columns fed with a recycled stream. The flushing fills the void volume, thereby ensuring effective removal of residual contaminants. Details of the process can be found in Zecca et al. (2025).

1.2. The CASOH technology

Calcium looping was extensively studied as a post-combustion CO_2 capture technology in conventional power plants and in biomass-driven systems. Its efficacy was also demonstrated in the reforming process for hydrogen production, showing significant benefits such as high CH_4 conversion and the production of high purity hydrogen at temperatures below 650°C (Masoudi Soltani et al., 2021; Yan et al., 2020). However, a critical challenge lies in the economic viability of $CaCO_3$ regeneration, a crucial step in the calcium looping process. The regeneration process requires temperatures exceeding 850°C and necessitates either pure oxygen from an air separation unit (Arias et al., 2013; Ströhle et al., 2014) or the integration of thermal storage mechanisms to effectively transfer heat from the carbonator to the calciner (Astolfi et al., 2021). Consequently, addressing the cost and energy demands of $CaCO_3$ regeneration is essential for the adoption of calcium looping technology.

An alternative approach, proposed by Abanades et al. (2010) and known as the calcium-copper (Ca-Cu) looping process, integrates calcium and chemical looping techniques using a copper based oxygen carrier. This method has been investigated as a potential solution for addressing the energy demands associated to calcination. An innovative system configuration called Calcium Assisted Steel mill Off-gas Hydrogen production (CASOH) incorporates Ca-Cu looping with the Sorption Enhanced Water Gas Shift (SEWGS) reaction. Fernández et al. (2020) and Grasa et al. (2023) explored this configuration, highlighting its potential to achieve high energy efficiency.

1.3. Aim of the work

The objective of this study is to evaluate the optimal integration of DISPLACE and CASOH technologies into the layout of a conventional BF-BOF steel plant, with the aim of minimizing the carbon footprint of steel production. The DISPLACE technology is applied to the flue gases generated by hot stoves, reheating furnaces, and sinter plant, while the CASOH technology is employed to process blast furnace gas and basic oxygen furnace gas, acting as a pre-combustion carbon capture solution. CASOH produces an H_2-rich mixture, which is utilized internally to generate steam. It is worth to underline that when H_2 is available in the steelmaking process it could be used as reducing agent, although, in this case, a H_2-N_2 separation step must be included. The CO_2 captured by both DISPLACE and CASOH can either be stored or used in the production of other goods. This study was carried out within the context of the C^{4}U project which aims to advance DISPLACE and CASOH from TRL 5 to 7. The project also includes extensive analyses of the economic, environmental, and business impacts of deploying CCUS in large-scale steel plants within the North Sea Port industrial cluster ("C4U website").

The paper is organised as follows: Section 2 gives details on the methodology adopted for the techno-economic assessment of the C^{4}U steel mill, describing the analysed plants, the modelling of the DISPLACE and CASOH technologies and their integration within a BF-BOF steel mill, as well as the assumption for the economic analysis and the KPIs; Section 3 shows the results; in Section 4 the conclusions are presented. Additional details about the methodology and the results are given in Appendix A, Appendix B and in the supplementary material.

2. Method

The methodology used for the techno-economic assessment of the C^{4}U steel mill is outlined in Figure 2. First, the base and reference BF-BOF steel plants, which served as the benchmarks for calculating key performance indicators (KPIs) were defined. Next, the layout of the C^{4}U steel mill was established, selecting the carbon capture technologies (DISPLACE and CASOH) to be integrated and determining the composition and mass flow rate of the gas to be treated in the carbon capture sections. A different gas distribution within the steel plant was chosen compared to the base case, introducing oxy-fired units to facilitate the post-combustion CO_2 capture in the DISPLACE columns. Simulations of

Table 2
BFG, BOFG and COG composition.

Gas stream	Composition [%mol]						
	CH_4	CO	CO_2	H_2	H_2O	O_2	N_2
BFG	-	21.79	20.54	2.30	4.00	-	51.36
BOFG	-	56.92	14.44	2.64	12.16	-	13.84
COG	23.24	3.87	0.97	60.05	3.15	0.19	5.82

the oxy-fired hot stoves, oxy-fired reheating ovens, and sinter plant with gas recirculation were performed to calculate the mass flow rate and composition of the flue gas to be fed to the DISPLACE technology. These data were input for simulating DISPLACE performance, conducted by TNO, the technology owner, using a Matlab code that models the DISPLACE technology. Multiple simulations were run to identify optimal operating conditions, targeting a carbon capture ratio (CCR) of 90 % and a CO_2 purity (CP) of 95 % (dry) at operating temperatures of 300, 350 and 400°C and pressures of 5, 6, 7, and 10 bar (Zecca et al., 2025). The results were integrated into the Aspen Plus model of DISPLACE within the steel plant. Separate Aspen Plus models were created for each of the three cases: decarbonization of flue gas from oxy-fired hot stoves, oxy-fired reheating ovens, and sinter plant. These models were used to define the heat exchanger network to recover waste heat and minimize additional fuel use for the carbon capture process. The Aspen Plus models were used also to calculate the electricity consumption of equipment like compressors and pumps required to compress the flue gas to the DISPLACE working pressure or the CO_2 stream to transport and storage pressure conditions. TNO's simulations also determined the size of the DISPLACE (column diameter and height), the number of columns per train, and the number of trains, which are essential for CAPEX estimation. KPIs typical of this analysis were computed helping to determine the optimal working conditions for each case. The methodology described in Zecca et al. (2025) was used to assess the performance of the DISPLACE technology under the previously mentioned operating conditions. While Zecca et al. (2025) provides specific details for the oxy-fired hot stoves case, the same approach was extended to evaluate the sinter plant and oxy-fired reheating furnace scenarios. Similarly, CASOH integration was performed and simulated in Aspen Plus permitting to find optimal operating condition of the CASOH technology and to carry out the techno-economic assessment of the C^4U steel plant. It should be also underlined that, in this work, no extra purification systems of the CO_2 streams produced by the carbon capture sections is considered. Further details are given in the following sections.

2.1. Analysed plants

The plants introduced in the description of the methodology are described in detail in the following sections. The base and reference steel mills are defined, respectively, as a state-of-the-art plant and a state-of-the-art steelmaking facility integrating a benchmark CO_2 capture technology.

2.1.1. Base BF-BOF plant

The base Blast Furnace-Basic Oxygen Furnace (BF-BOF) steel mill analysed in this study was modelled using as reference the plant described in IEAGHG Technical Report (2013), with modifications, such as the plant size (in this study set to 3.16 Mt_{HRC}/y) and slight variations in the composition of blast furnace gas (BFG), whose average composition, was provided by an industrial partner of the C^4U project consortium, based on data from an existing facility (Khallaghi et al., 2022). On the other hand, the compositions of BOFG and COG indicated in IEAGHG Technical Report (2013) were used. Table 2 provides details on the composition of BFG, BOFG, and COG. All sections of the steel plant have been modelled to ensure an accurate carbon balance across the entire facility.

Table 3
Main results of the WGS + MDEA pre-combustion carbon capture section.

Parameter	Unit	Value
CO_2 capture rate	%	85
CO_2 to storage	t/h	310
MDEA/water content in the lean solvent	%wt	25/72
Lean solvent/$CO_{2,in}$	(kg/h)/(kg/h)	21.82
Lean solvent CO_2 loading	mol_{CO2}/mol_{MDEA}	0.05
Rich solvent CO_2 loading	mol_{CO2}/mol_{MDEA}	0.51
Reboiler duty	MW	116
Reboiler specific duty	GJ/t_{CO2}	1.34
Power consumption (including CO_2 compression)	MW	35.71
Steam pressure from MP steam turbine	bar	6
Natural gas fired boiler duty	MW	71.6
Natural gas consumption for auxiliary steam production	kg/h	5817

The definition of gas distribution within the base steel plant is pivotal for conducting the techno-economic assessment of integrating carbon capture technologies. This distribution governs the composition and mass flow rates of exhaust gases from various sections of the plant, which are crucial considerations for implementing post-combustion carbon capture technologies or for determining the flow rates of steelmaking gases to be decarbonized (such as BFG, BOFG, COG) when employing pre-combustion carbon capture technologies.

2.1.2. Reference BF-BOF plant

In a steel plant there are numerous emission points that contribute to the overall emissions of the facility. Studies found in the literature typically focus on decarbonizing just one of these fluxes. Given that flue gas from the power plant accounts for about 50 % of the total CO_2 emissions, decarbonization options for this gas stream are evaluated by Khallaghi et al. (2022) and Manzolini et al. (2022). The reference plants considered in this work integrate a commercially ready carbon capture technology (MDEA pre-combustion CO_2 absorption system), thus the methodology and plant layout presented by Khallaghi et al. (2022) is adopted. The primary difference lies in the composition and mass flow rate of the gas being decarbonized; in this work, a mixture of blast furnace gas (BFG) and basic oxygen furnace gas (BOFG) is used as fuel in the power plant, whereas in Khallaghi et al. (2022) only BFG is considered.

BFG and BOFG mixture is firstly compressed to 3 bar and then converted into H_2 + CO_2-rich gas in the WGS stage, reacting with steam. Steam, available at 6 bar is heated to 330°C and then introduced into the WGS reactor. The shifted gas is cooled to 355°C to pre-heat the WGS feed mixture. Before entering the absorber column, the shifted gas is further cooled to 40°C, and the condensed water is removed. In the absorber column, the syngas comes into contact with the lean solvent (MDEA) that absorbs the CO_2. A decarbonized clean fuel exits at the top of the absorber column, while the CO_2-rich solvent exits from the bottom. The rich solvent is pumped to 6 bar and heated to 80°C before entering the stripping column. The lean solvent leaves the bottom of the stripper, is expanded to 2 bar, cooled to 40°C, and then fed to the top of the absorber. High-purity CO_2 exits the top of the stripper column, with evaporated water removed in a condenser. The CO_2-rich stream is then compressed to 78 bar in a multistage compressor, liquefied by cooling to 25°C, and pumped to 110 bar. The simulation of the carbon capture plant has been carried out in Aspen Plus V14 and the ELECNRTL method has been selected, being this method typically employed in this kind of simulations (Antonini et al., 2021; Khallaghi et al., 2022; Mudhasakul et al., 2013), using as reference the plant scheme shown in Khallaghi et al. (2022) and the methodology described in Zecca et al. (2023).

All the steam necessary for the WGS reaction is taken from the power plant's steam cycle at the exit of the medium-pressure steam turbine.

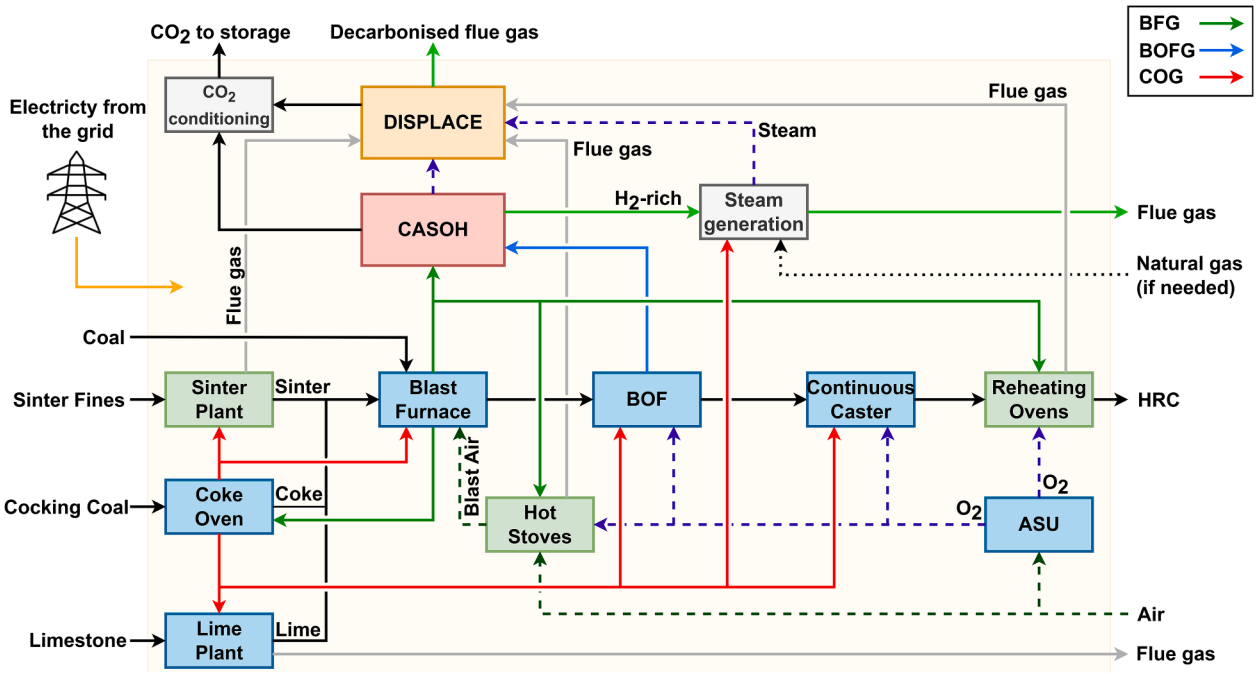

Fig. 3. C^{4}U steel plant simplified layout.

Similarly, part of the steam used for solvent regeneration in the reboiler is sourced from the power plant. Therefore, the low-pressure steam turbine is not present in the steam cycle of the reference BF-BOF plant, as all the steam at the exit of the medium-pressure steam turbine is diverted to the carbon capture section. The condensate is then sent back to the heat recovery steam generator. The electricity generated in the power plant is thus reduced in comparison with the base case. Additional steam has to be supplied to the reboiler, assuming to be generated in a natural gas-fired boiler. The efficiency of the combined cycle, simulated in Aspen Plus V14, is 41.29 %, generating 152.25 MW against a demand of 190.16 MW. Table 3 details the main results of the simulation of the CO_2 capture section for the reference steel plant.

2.1.3. *C^{4}U steel plant*

In the C^{4}U steel plant, two different technologies are integrated to reduce plant emissions. The DISPLACE technology is employed to decarbonize the flue gas from three units: the reheating ovens, the hot stoves, and the sinter plant, while the CASOH technology, a pre-combustion carbon capture technology, produces a hydrogen-rich stream from BF and BOF gases. As shown in Fig. 3, an alternative gas distribution was proposed compared to the base steel mill (IEAGHG Technical Report, 2013) to optimally accommodate the CO_2 capture technologies within the steel plant. Coke oven gas, responsible for approximately 6 % of the overall CO_2 emissions in the base case, was identified as a suitable fuel to supply the energy demand of the CO_2 capture system. Due to its internal availability and high content of H_2 and CH_4, COG was utilized for steam generation required by the DISPLACE process. Consequently, BFG replaces COG in units such as hot stoves and reheating ovens, where COG is typically employed as fuel. Various options were evaluated, considering the feasibility of adopting oxy-fired units like oxy-fired hot stoves or oxy-fired reheating ovens. Oxy-fired units offer the advantage of generating more concentrated CO_2 in the flue gases, thereby facilitating the adsorption process in the DISPLACE columns. However, a drawback is the need for a larger air separation unit to produce the additional oxygen. These units use blast furnace gas as fuel instead of coke oven gas, possible because of the absence of a power plant. Consequently, all electricity for the C^{4}U steel mill must be imported from the grid. CASOH technology provides the advantage of producing extra steam and a hydrogen-rich stream suitable for steam generation in the DISPLACE process. Several configurations involving single or multiple DISPLACE units were considered. Priority was given to using coke oven gas as the primary fuel source to fulfil the additional heat requirements for the DISPLACE CO_2 capture process, while exporting the H_2-rich stream from CASOH. If COG proves insufficient to meet the DISPLACE heat demand, the hydrogen-rich stream serves as additional fuel, with any excess being exported.

2.2. *DISPLACE modelling and process integration*

In a conventional BF-BOF steel mill, iron-bearing materials such as iron ore lump, sinter, and pellets are reduced to metallic iron in the blast furnace. These materials, along with additives like limestone and reducing agents such as coke, are introduced from the top of the furnace. Additionally, hot blast air enriched with oxygen is injected into the lower section of the furnace, promoting the formation of carbon monoxide from coke, which subsequently reduces the iron ores to metallic iron (Remus et al., 2013). Hot stoves function as high-temperature heat exchangers that heat cold ambient air to a required temperature (900 – 1350°C) through a cyclical process. Typically, a combination of blast furnace gas and coke oven gas serves as fuel to generate hot combustion gases. These gases circulate through a network of heat-resistant refractory pipes and chambers until the materials reach the necessary temperature (1100 – 1500°C). At this point, the combustion gases are cut off, and cold ambient air is introduced in the opposite direction. The heat stored in the refractory bricks is transferred to the incoming air. This cycle repeats until the blast air reaches the target temperature, triggering the start of a new cycle (Remus et al., 2013). The implementation of oxy-fired hot stoves has been proposed for the C^{4}U steel plant. In this approach, only BFG is used as fuel, and it is combusted with oxygen instead of air. This modification reduces BFG consumption while increasing CO_2 concentration in the flue gases, thereby enhancing the efficiency of the carbon capture process.

The performance of blast furnaces is enhanced by the prior preparation of the burden in the sinter plant. Iron-bearing materials, such as iron ores and recycled materials from downstream operations (coarse dust, sludge from blast furnace cleaning, mill scale, etc.), are agglomerated with additives (quartzite, olivine, limestone, lime) and fuels (coke breeze). This operation improves the mechanical and

Table 4
Flue gas streams processed by DISPLACE with corresponding thermodynamic conditions.

Flue gas	ṁ [kg/s]	T [°C]	P [bar]	Composition [%mol]					
				CO_2	CO	O_2	N_2	Ar	H_2O
RO	78.66	500	1.03	41.90	-	1.00	50.81	0.04	6.25
HS	87.88	140	1.03	41.90	-	1.00	50.81	0.04	6.25
SP	123.99	120	1.03	16.84	0.32	4.00	64.15	-	14.69

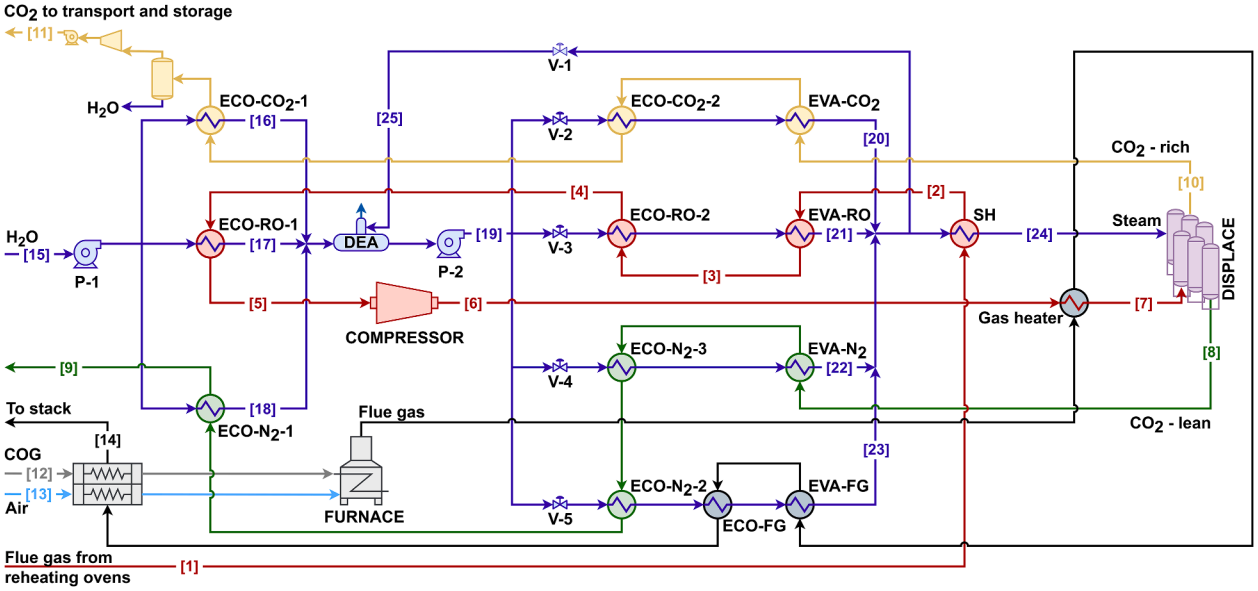

Fig. 4. Plant scheme of the integration of DISPLACE technology for decarbonisation of flue gas from reheating ovens.

metallurgical properties of the burden, producing a product characterized by high porosity, stable chemical composition, and constant melting behaviour (Niel et al., 2022; Remus et al., 2013). The raw materials are first collected and prepared in precise quantities, then mixed in a rotary drum with water addition. This mixture is subsequently placed on top of a 30 – 50 mm layer of recycled sinter on a large traveling grate. At the beginning of the grate, the sintering reaction is initiated by burners that ignite the coke breeze. Process air is drawn by blowers into distribution chambers, known as windboxes, located underneath the grate. At the end of the grate, the produced sinter is crushed, cooled, and divided into three fractions. The sinter fines are recirculated, the second fraction is used as a hearth layer, and the remaining part is used in the blast furnace (Niel et al., 2022; Remus et al., 2013). Exhaust gas from the sinter plant represents a significant share of the emissions of the entire steel mill, accounting for about 14 % of the base BF-BOF steel plant emissions. These gases also contain compounds such as heavy metals (particularly iron and lead compounds), alkali chlorides, sulphur oxides, NO_x, hydrogen chloride, hydrogen fluoride, hydrocarbons, polycyclic aromatic hydrocarbons (PAHs), and aromatic compounds. Being the aforementioned pollutants present in the order of magnitude of ppm they are not considered in this work. The typical composition of flue gas from the sinter plant is taken from IEAGHG Technical Report (2013). The CO_2 molar fraction is typically low, around 5 %. This level is too low for efficient CO_2 capture in the DISPLACE columns, so a recirculation of the waste gas is proposed. Consequently, the composition of the exhaust gas from the sinter plant was computed with the objective of reducing the oxygen molar fraction to 4 %, as indicated by industrial partners within the C^4U project consortium, resulting in a CO_2 molar fraction above 16 % (Table 4).

The reheating furnaces are used in hot rolling mills to heat steel stocks (billets, blooms, or slabs) to approximately 1200°C, a temperature suitable for the plastic deformation of steel, thus facilitating the rolling process. In the base steel mill, COG is used as fuel to heat the slabs in the walking beam furnaces. The adoption of oxy-fired reheating ovens was proposed for the C^4U steel plant using BFG as fuel. Similarly to the oxy-fired hot stoves, this increases the concentration of CO_2 in the flue gases, effectively enhancing the carbon capture process.

The optimal integration of DISPLACE technology into the steel mill layout was carried out considering various operating conditions in terms of temperature (300, 350 and 400°C) and pressure (between 5 – 10 bar), focusing on scenarios in which the CO_2 capture rate exceeds 90 % while ensuring a minimum CO_2 purity of 95 % (Zecca et al., 2025). Through comprehensive simulations of the DISPLACE cycles, key parameters, such as number and size of the columns, number of trains, CCR, CO_2 purity, steam consumption, were accurately computed.

The lay-out of the DISPLACE integration for the decarbonisation of the reheating oven flue gases is reported in Figure 4. In the case of flue gas from hot stoves and sinter plant a similar but less complex scheme was adopted, as detailed in Zecca et al. (2025). This is due to the different temperature at which the flue gases are available. The flue gases, which composition is reported in Table 4, are typically slightly above atmospheric pressure. Before compression, they are cooled to 35°C to minimize compression work, also contributing to pre-heat a portion of the water used for generating steam (utilized in the DISPLACE columns) up to 102°C. Steam is generated at pressure and temperature matching the operating conditions of the DISPLACE unit. In the case of flue gas from reheating ovens, the high temperature (500°C) permits to generate part of the steam necessary for the carbon capture process. Similarly, the outlet gas streams from the DISPLACE process, the CO_2-rich stream and the CO_2-lean gas stream, are cooled, generating steam. A furnace is employed to supply heat to the gas stream exiting the compressor and to superheat the steam to the DISPLACE working temperature. This furnace can alternately use natural gas, coke oven gas or

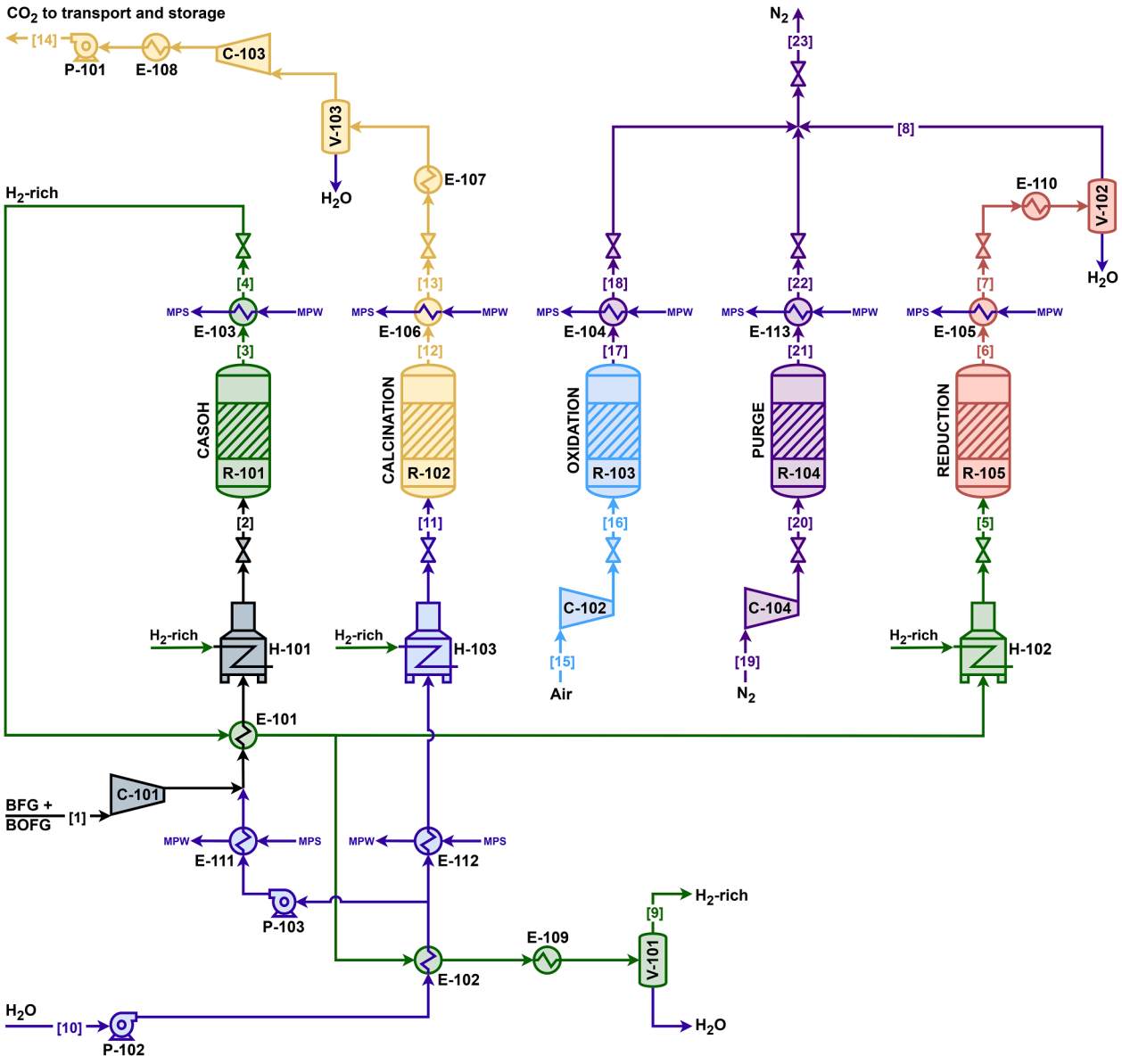

Fig. 5. Process flow diagram of the CASOH process.

the H_2-rich stream from CASOH as fuels. Prior to entering the furnace, the fuel and combustion air are preheated by the furnace flue gases. To prevent the presence of non-condensable species in the steam, a deaerator is included. The CO_2-rich stream is brought to the conditions for transport and storage through a multistage compressor, reaching pressures of up to 78 bar, then being liquefied at 25°C and finally pumped to a pressure of 110 bar as described in Wright et al. (2011) and in Zecca et al. (2023). The specifications of the streams indicated in Fig. 4 are given in Table A.1 (Appendix A). Since many different operating conditions of DISPLACE were analysed, only the results regarding the case 5 bar – 400°C are shown as an example.

Simulations of DISPLACE integration were performed in Aspen Plus 14 using the RKS-BM property method, starting from a detailed DISPLACE model developed by TNO and described in Zecca et al. (2025).

2.3. CASOH modelling and process integration

CASOH process flow diagram is shown Figure 5. A mixture of blast furnace gas and basic oxygen furnace gas is transformed into a H_2-rich stream through five primary steps (i.e., CASOH reaction, calcination, oxidation, purge and reduction) conducted in multiple packed-bed reactors operating in parallel. These reactors dynamically alternate between different temperatures and pressures to suit each step's requirements (Fernández et al., 2020).

In the CASOH step, the gas mixture is first compressed to 10 bar and mixed with steam, maintaining a steam-to-CO ratio of 2. Before entering the CASOH reactor, the gas mixture is heated to around 520°C in a furnace by burning a fraction of the H_2-rich gas produced by the reactor. Inside the reactor, the water-gas shift reaction occurs, catalysed by Cu-based particles, producing H_2 and CO_2. Simultaneously, CaO sorbent reacts with both the generated CO_2 and the CO_2 initially present in the gas through carbonation, forming $CaCO_3$. This carbonation shifts the equilibrium toward increased H_2 production by continuously removing CO_2 from the gas phase, achieving a high CO conversion equal to 99 % and yielding a gas stream rich in H_2 (around 30 % by volume) (Abbas et al., 2022; Grasa et al., 2023). The exothermic reactions of WGS and carbonation raise the temperature of the bed to around 750°C. The outlet gas stream is cooled down to 210°C with saturated water at 12 bar and 190°C, generating MP steam.

Table 5
Operating conditions of CASOH reaction stages used in the process modelling.

Stage	P [bar]	T [°C]	Reactions
CASOH	9.7	750	$CO + H_2O \rightarrow CO_2 + H_2$ $CaO + CO_2 \rightarrow CaCO_3$
Calcination	0.5	833	$CaCO_3 \rightarrow CaO + CO_2$
Oxidation	10	603	$Cu + 1/2O_2 \rightarrow CuO$
Purge	9.5	603	
Reduction	8.5	677	$CuO + H_2/CO \rightarrow Cu + H_2O/CO_2$

In the calcination step, the reactor bed is depressurised under mild vacuum conditions (0.5 bar) and high-temperature steam (525°C and 3 bar) is fed into the reactor. The heat generated during the preceding exothermic WGS and carbonation reactions is stored in the solid bed material inside the reactor later used to support the endothermic calcination reaction. Additional heat is nevertheless needed, and this is supplied by the H_2-rich gas combustion. The reactor bed temperature increases to 833°C, and a high-purity CO_2 stream (over 99 % by mol) is released through $CaCO_3$ calcination. The outlet gas stream is then cooled down to 210°C with saturated water at 12 bar and 190°C, generating MP steam.

In the oxidation step, air is introduced into the reactor and reacts with the metal-based particles (primarily Cu), oxidizing them to CuO. The exothermic reaction rapidly increases the bed temperature to around 600°C, ensuring fast and complete O_2 conversion. High pressure (10 bar) and moderate temperatures minimize CO_2 release from any partial calcination of $CaCO_3$. The product gas is mainly N_2 (over 99 % by mol) and this stream is cooled down to 210°C with saturated water at 12 bar and 190°C, generating MP steam.

After the oxidation, a purge step is implemented using nitrogen. Nitrogen, which is an inert gas, enters the reactor at approximately 10 bar and 190°C and sweeps the oxygen present as it flows through the bed. This process prepares the reactor for the next stage and allows for the recovery of high temperature heat, as the gas outlet is cooled from 603°C to 210°C, producing MP steam.

Finally, in the reduction step, around 15 % of the H_2-rich stream from the CASOH reacts with CuO, converting it back to Cu. The reduction reaction regenerate the catalyst and lead to additional CO_2 and H_2O production. The outlet gas is cooled down to 210°C with saturated water at 12 bar and 190°C, generating MP steam. The specifications of the streams shown in Fig. 5 are given in Table A.1.

The performance of the CASOH process was evaluated using a multi-step modelling approach. First, the five distinct reaction and heat recovery stages were simulated using a detailed 1-D dynamic reactor model (Abbas et al., 2021). This model integrates mass transfer limitations, reaction kinetics, and comprehensive energy balances to predict the time-dependent profiles for product gas compositions and temperatures for a single packed-bed reactor completing a full operational cycle. To assess the overall performance and integration of the CASOH system within the steel plant, these dynamic outputs were then used to construct a steady-state process model in Aspen Plus. This is achieved by representing each key stage (e.g., the CASOH, calcination, etc.) with separate, steady-state unit operation blocks (0-D models). The inputs for these blocks, such as flow rates and compositions, are derived from the representative outputs generated by the 1-D model for each stage, so that the overall plant can achieve a pseudo-continuous and stable output (Abbas et al., 2021; Fernández et al., 2020). The operating conditions of the CASOH stages are given in Table 5. Key uncertainties and simplifications in this approach include: switching and purging losses (e.g., the model does not account for the material or energy losses that occur during the finite time required for valves switching and reactor purging), thermal dynamics (e.g., does not fully capture heat losses during standby periods or the dynamic response of the heat recovery loops), and process control (e.g., the model assumes perfect scheduling and does not include the buffering that would be required in a real plant to smooth out minor fluctuations in flow and composition from the cycling reactors) (Fernández et al., 2020; Grasa et al., 2023).

Table 6
Property methods and Aspen Plus components used in the process modelling.

Plant section	Aspen Plus ID	Comments / Specifications
DISPLACE - (RKS-BM property method)		
DISPLACE	Sep	A calculator block computes the mass flow rate and composition of the outlet streams
Flue gas compressor	MCompr	2 stage; $\eta_{p,1,2} = 0.8$; $\eta_m = 0.95$; $T_{intercooling} = 50°C$
Deaerator	Flash2	
Furnace	RGibbs	
Gas-gas heat exchanger	HeatX	Minimum ΔT gas-gas heat exchanger = 15°C
Pumps	Pump	$\eta_h = 0.75$; $\eta_m = 0.95$
CASOH - (PENG-ROB property method)		
CASOH reactor	RStoic + RGibbs	RStoic used to define 99 % conversion of CO to CO_2 and H_2; RGibbs used to calculate phase and chemical equilibrium in the reactor products
Calcination reactor	Heater	Temperature 833°C
Oxidation reactor	Heater	Temperature 603°C
Reduction reactor	RStoic	Fractional conversion 100 % of CO and H_2 to CO_2 and H_2O
BFG + BOGF compressor	MCompr	3 stages; $p_{out} = 10.8$ bar; $\eta_{p,1,2,3} = 0.75$; $\eta_m = 0.95$; $T_{intercooling} = 30°C$; $\Delta p_{intercooler,1,2} = 0$ bar
Air compressor	MCompr	2 stages; $p_{out} = 10.6$ bar; $\eta_{p,1,2} = 0.75$; $\eta_m = 0.95$; $T_{intercooling} = 30°C$; $\Delta p_{intercooler,1} = 0$ bar
N_2 compressor	MCompr	2 stages; $p_{out} = 9.5$ bar; $\eta_{p,1,2} = 0.75$; $\eta_m = 0.95$; $T_{intercooling} = 40°C$; $\Delta p_{intercooler,1} = 0$ bar
Furnaces	Heater	A fraction of the H_2-rich gas from CASOH-reactor is burned
Pumps	Pump	$\eta_h = 0.75$; $\eta_m = 0.95$
Reactor outlet coolers	Heater	Cooling fluid: saturated water at 12 bar and 190°C; MP steam is generated
CO_2 compression train - (RKS-BM property method)		
CO_2 compressor	MCompr	3 stages; $p_{out} = 80$ bar; $\eta_{p,1,2} = 0.8$; $\eta_{p,3} = 0.75$; $\eta_m = 0.95$; $T_{intercooling} = 28°C$; $\Delta p_{intercooler,1} = 0.05$ bar; $\Delta p_{intercooler,2} = 0.19$ bar
CO_2 pump	Pump	Discharge pressure = 110 bar; $\eta_h = 0.75$; $\eta_m = 0.95$
MDEA CC capture sections - (ELECNRTL property method)		
WGS	RGibbs	p = 3 bar; duty = 0; calculate phase equilibrium and chemical equilibrium
Absorber	RadFraq	Equilibrium; 20 stages; condenser: none; reboiler: none
Stripper	RadFraq	Equilibrium; 20 stages; condenser: partial-vapor-liquid; reboiler: Kettle
Regenerative heat exchanger	HeatX	Pinch point ΔT = 10°C
Pump	Pump	Discharge pressure = 6 bar; $\eta_h = 0.75$; $\eta_m = 0.95$
Expander	Compr	Discharge pressure = 110 bar; $\eta_{is} = 0.85$; $\eta_m = 0.95$
Waste heat recovery - (STEAMNBS property method on water/steam side)		
Economiser; evaporator; superheater	HeatX	Minimum ΔT gas-liquid heat exchanger = 10°C; economizer ΔT subcooling = 5°C; economizer hot-side pressure drop = 0.2 bar; economizer cold-side pressure drop = 0.7 bar; evaporator hot-side pressure drop = 0.2 bar

2.4. Plants modelling

This section summarizes the methodology used for the modelling of the plants aforementioned. Table 6 details the property methods selected for each case, along with the Aspen Plus unit operation blocks for the primary equipment in each plant. Additional minor equipment,

Table 7
Assumptions for the thermodynamic assessment.

Parameter	Unit	Value
Steel plant capacity	Mt_{HRC}/y	3.16
Plant availability	h/y	8200
NG LHV	MJ/kg	46.87
COG LHV	MJ/kg	40.21
Electricity CO_2 emissions	kg_{CO2}/MWh_{el}	250
Water recovery from CO_2 stream	%	90

Table 8
Equipment reference cost.

Component	Scaling parameter	C_0 [M€]	S_0	f	Reference
CO_2 capture unit (MDEA)	CO_2 mass flow rate [t/h]	10.52	12.4	0.60	(Cormos et al., 2020b)
CO_2 compressor and condenser	Power [MW]	55.24	50.5	0.67	(Manzolini et al., 2020)
Furnace	Heat duty [MW]	0.30	1.00	1.00	(Khallaghi et al., 2022)
Compressor	Power [MW]	10.17	15.3	0.67	(Manzolini et al., 2020)
Pump	Volumetric flow [m^3/h]	0.28	250	0.14	(Huijgen et al., 2007)
WGS	H_2 and CO flow rate [kmol/s]	3.89	1.68	0.67	(Manzolini et al., 2020)
Gas turbine	Power [MW]	62.02	272.1	0.67	(Manzolini et al., 2020)
Steam turbine	Power [MW]	41.43	200	0.67	(Manzolini et al., 2020)
Heat exchanger	Heat transfer [MW]	16.25	138	0.67	(Guo et al., 2014)

Table 9
Assumptions common to all plants for the economic assessment.

Parameter	Unit	Value
Currency exchange	€/$	0.92
NG/BFG/BOFG/COG buying/selling price	$€/MWh_{LHV}$	50
Electricity price	$€/MWh_{el}$	125
Electricity selling price	$€/MWh_{el}$	1/3•El. price
Discount rate	%	8.00
Lifetime	years	25
Fixed Charge Factor	%	9.37
Water cost	$€/m^3$	1
Personnel annual salary	€/y	60000
Total Installation Cost	% TEC	104
Indirect Costs	% (TEC+TIC)	14
Contingency	% (TEC+TIC+IC)	10
Owner's Costs	% (TEC+TIC+IC)	5
CO_2 transport and storage	$€/t_{CO2}$	40
CO_2 tax	$€/t_{CO2}$	0
N° additional employees per CC section	-	15
Maintenance cost for CO_2 capture section in BF-BOF plant	% $TPC_{CC\ section}$	2.5
DISPLACE maintenance costs	% $TPC_{DISPLACE\ CC}$•FCF	5

such as mixers, splitters, valves, reactors, pumps, compressors, and heat exchangers, are also utilized in the plant simulations.

General assumption used in the techno-economic assessment and common to all the plants analysed are shown in Table 7.

2.5. Methodology for the economic assessment

This section summarizes the key assumptions used to perform the economic assessment. The methodology adopted to calculate the capital costs is based on bottom-up approach starting from the Total Equipment Cost (TEC) and computing the Total Annual Cost (TAC) as described in Khallaghi et al. (2022), Manzolini et al. (2020) and in Zecca et al. (2023). The CEPCI index, computed as the average between the years 2019 and 2022 (equal to 712.47) was used to update the cost of equipment found in literature. Table 8 summarizes the updated reference cost of equipment used to carry out the economic assessment. Table 9 lists the general assumptions that are common across all cases evaluated. Electricity and natural gas prices are crucial factors influencing operational costs. The prices used in the assessment were derived from data reported in "International industrial energy prices - GOV.UK", reflecting average values for the European Union between 2019 and 2022. Specifically, annual industrial electricity prices, inclusive of environmental taxes and levies for very large consumers, were considered. Similarly, annual industrial natural gas prices, including taxes for large consumers, were used.

The cost of CO_2 transport and storage for this study is set at 40 $€/t_{CO2}$. This figure aligns with estimates provided by Smith et al., who suggest a range of 4 and 45 $\$/t_{CO2}$ depending on factors such as transport distance, scale (i.e. quantity of CO_2 transported and stored), monitoring assumptions, reservoir geology and pipeline capital costs (Smith et al., 2021).

In the case of C^4U steel mill, as detailed in section 2.3 the CASOH unit generates a H_2-rich stream and steam. Any surplus of hydrogen is assumed to be sold at a price equivalent to the levelized cost of blue hydrogen (LCOH) produced via steam methane reforming. The National Energy Technology Laboratory (NETL) indicates the variation of LCOH with respect to natural gas price for NG prices ranging from 1 to 10 \$/MMBtu equivalent to 3.14 and 31.39 $€/MWh_{LHV}$ (Lewis et al., 2022). For the purposes of this study, the data were extrapolated to encompass NG prices up to 100 $€/MWh_{LHV}$ (or 31.86 \$/MMBtu). The relationship between hydrogen cost and NG price is represented by a linear equation derived from the plotted data, adjusted here for NG prices (C_{NG}) in $€/MWh_{LHV}$:

$$\mathrm{LCOH}\left[€\Big/ kg_{H_2}\right] = 0.7513 + 0.05373 \times C_{NG} \quad (1)$$

In the context of the CASOH technology, the economic assessment was conducted based on data gathered from vendors during the C^4U project. Data included the cost of the main process equipment (e.g., reactors, compressors, furnaces, heat exchangers, pumps) estimated based on the equipment size and material of construction. The base cost of equipment (for a reference size or capacity) was updated using a scaling factor of 0.7 and a reference property (e.g., duty for furnaces, power for compressors, etc.). The CASOH plant is designed to process the gas mixture (BFG + BOFG) in 4 trains. Each train has 16 reactors: 7 are used for the CASOH reaction, 6 for calcination, 1 for oxidation, 1 for reduction and 1 for purge. Each reactor has 5 valves at the inlet and the outlet, which are used to dynamically alternate between the different CASOH stages. The list of equipment and its cost are included in Table 2 in the supplementary material.

The methodology used for computing the total equipment cost of the DISPLACE units is described in Zecca et al. (2025).

2.6. Key performance indicators

The comparison across all investigated cases is conducted using economic and environmental Key Performance Indicators (KPIs), commonly referenced in literature (Gentile et al., 2022; Khallaghi et al., 2022; Manzolini et al., 2020). The environmental indexes considered include the primary energy consumption (PEC), the specific CO_2 emissions (e_{CO2}), the CO_2 capture ratio (CCR), SPECCA and CO_2 avoidance (CA).

$$\mathrm{PEC}\left[\frac{GJ_{LHV}}{t_{HRC}}\right] = \frac{\dot{m}_{fuel}LHV_{fuel} + PEC_{el} + \dot{Q}_{req}/\eta_{th}}{\dot{m}_{HRC}} \quad (2)$$

Table 10
PEC of electricity generation.

Parameter	Unit	RES	NGCC
Electricity C.I.	kg_{CO2}/MWh_{el}	0	350
Cycle efficiency	MW_{el}/MW_{LHV}	-	60
PEC electricity generation	MWh_{LHV}/MWh_{el}	0	1.67

$$e_{CO_2}\left[\frac{t_{CO_2}}{t_{HRC}}\right] = \frac{\dot{m}_{CO_2}}{\dot{m}_{HRC}} \quad (3)$$

$$CCR\ [\%] = \frac{(\dot{m}_{CO_2})_{CO_2-product}}{(\dot{m}_{CO_2} + \dot{m}_{CO})_{feed}} \cdot 100 \quad (4)$$

$$SPECCA\left[\frac{GJ_{LHV}}{t_{CO_2}}\right] = \frac{PEC_{capture} - PEC_{no\ capture}}{e_{CO_2,no\ capture} - e_{CO_2,capture}} \quad (5)$$

$$CA\ [\%] = \frac{e_{CO_2,no\ capture} - e_{CO_2,capture}}{e_{CO_2,no\ capture}} \cdot 100 \quad (6)$$

In this study, the primary energy consumption (PEC) associated with electricity generation varies on the basis of its CO_2 footprint. Values provided in Table 10 serve as reference points, with linear interpolation used for intermediate scenarios. In the renewable energy scenario, with a carbon intensity of 0 kg_{CO2}/MWh_{el}, since no fossil fuel are consumed during operation, the PEC related to electricity generation is considered as 0 MWh_{LHV}/MWh_{el}. On the other hand, when the electricity carbon footprint reaches 350 kg_{CO2}/MWh_{el}, it is assumed that the electricity is produced in a natural gas combined cycle (NGCC) plant with an efficiency of 60 %.

The economic performance is assessed computing the levelized cost of hot rolled coil (LCOHRC) and the cost of CO_2 avoidance (CCA). The total annualized cost (TAC) is calculated according to equation (7) using the methodology described in Khallaghi et al. (2022), Manzolini et al. (2020) and in Zecca et al. (2023) starting from the computation of the total equipment cost.

$$TAC\left[\frac{M€}{y}\right] = TPC \cdot FCF + C_{f,O\&M} + C_{v,O\&M} - Revenues \quad (7)$$

$$LCOHRC\left[\frac{€}{t_{HRC}}\right] = \frac{TAC}{\dot{m}_{HRC} \cdot h_{eq}} \cdot 10^6 \quad (8)$$

$$CCA\left[\frac{€}{t_{CO_2}}\right] = \frac{LCOHRC_{capture} - LCOHRC_{no\ capture}}{e_{CO_2,no\ capture} - e_{CO_2,capture}} \quad (9)$$

To ensure a fair comparison among all the plant configurations analysed in this study and to account for differences in the import and export of commodities, the following assumptions have been made. For electricity export, such as in the case of the base BF-BOF plant, reductions in emissions and primary energy consumption are considered. These reductions are calculated based on the specific scenario chosen for the carbon footprint of electricity generation, using the values outlined in Table 10. Similarly, when exporting gas streams like COG and H_2-rich mixture or steam, reductions in emissions and primary energy consumption are also taken into account by computing the equivalent amount of NG on energy basis, which is assumed to be the fuel being replaced. Exporting electricity effectively means that another user does not need to purchase the equivalent amount of electricity from the grid, which would have its own associated carbon footprint and primary energy consumption based on the electricity generation scenario considered. Likewise, exporting COG, hydrogen or steam means that the purchaser does not need to buy an equivalent amount of natural gas which, in this study, is considered the baseline fuel that would otherwise be consumed.

Table 11
Electricity and fuel consumption of DISPLACE units.

Parameter	Unit	Reheating ovens	Hot stoves	Sinter plant
Working pressure	bar	5	5	5
Working temperature	°C	400	400	400
Columns diameter	m	3	3	3
Number of columns per train	-	6	6	6
Number of trains	-	4	4	3
Steam to carbon	mol_{H2O}/mol_{CO+CO2}	2.18	2.18	3.59
CO_2 capture rate	%	90.38	90.38	90.43
CO_2 purity (dry)	%	95.41	95.41	95.05
Emissions if without CO_2 capture	t_{CO2}/t_{HRC}	0.397	0.444	0.298
El. consumption for flue gas compression	MW_e	23.20	16.00	27.21
El. consumption for CO_2 compression	MW_e	10.19	11.28	7.59
Total electricity consumption	MW_e	33.39	27.28	34.80
Fuel consumption	MW_{th}	58.26	103.14	113.20

Table 12
Thermodynamic performance of CASOH when simultaneously integrated with DISPLACE.

Parameter	Unit	No capture	CASOH
Total BFG + BOFG input	MW_{LHV}	226.9	226.9
Thermal energy output	MW_{LHV}	226.9	169.5
Cold gas efficiency	%	100.0	74.7
Net power consumption	MW_{el}	-	57.9
Heat requirement	MW_{th}	-	61.3
CO_2 flow rate for storage	kg/s	-	51.6
CO_2 purity for storage	%	-	99.8
CO_2 emission	kg/s	56.5	4.8
CO_2 capture efficiency	%	-	91.5
Specific CO_2 emission	kg_{CO2}/GJ_{LHV}	248.8	28.4
Specific CO_2 emission	kg_{CO2}/t_{HRC}	527.4	45.0
Steam produced	MW	-	31.4
H_2-rich mix produced	kg/s	-	34.7
H_2-rich mix used for heat requirement	kg/s	-	13.3
H_2-rich mix available	kg/s	-	21.4
H_2-rich mix LHV	MJ/kg	-	4.89

3. Results

In this section the performance of the CASOH and DISPLACE units as well as the results of the techno-economic assessment of the C^4U steel mill are shown.

3.1. DISPLACE performances

As mentioned in previous sections multiple simulations of DISPLACE units were performed, considering different values of DISPLACE operating temperature and pressure. Table 11 presents, for the three considered applications of DISPLACE, the results of the cases showing the lowest cost of CO_2 avoided across the simulations performed. These results were obtained considering the reference values of the natural gas and electricity prices, as well as of the CO_2 footprint associated with electricity imported from the grid.

3.2. CASOH performances

The performance of CASOH processing a mixture of BFG and BOFG are given in Table 12. These data were used for the techno-economic assessment of C^4U steel mill as shown in section 3.3. The CASOH unit, produces a steam stream that can be used in the DISPLACE units, reducing the consumption of fuel for steam production.

Table 13
BFG and COG consumption in non-oxy-fired units.

Fuel	Non-oxy-HS	Oxy-HS	Non-oxy-RO	Oxy-RO
BFG (dry) [kg/s]	77.22	77.22	69.12	69.12
COG (wet) [kg/s]	0.333	-	0.278	-

3.3. Overall plant performance and emissions for different level of integration

This section presents the results of the C^{4}U steel plant with the simultaneous integration of CASOH and DISPLACE technologies. Similar to the base case, the C^{4}U steel mill consumes 4845 t/day of coking coal in the coke plant and 1473 t/day of PCI coal in the blast furnace. The plant's electricity requirements are met by importing electricity from the grid, as there is no on-site power plant.

Different levels of integration of carbon capture technologies are presented and compared to the base and reference BF-BOF plants, including the integration of CASOH technology alone and with the addition of DISPLACE to single or multiple units. When DISPLACE is integrated alongside CASOH, the graphs only indicate the steel mill section(s) equipped with DISPLACE, denoted as "HS", "RO" and "SP" for hot stoves, reheating ovens and sinter plant, respectively. In addition, the adoption of oxy-fired units, such as hot stoves and reheating ovens, is considered only when DISPLACE technology is implemented to decarbonize the flue gas from these sections. Oxy-fired units necessitate the installation of a larger air separation unit, which increases both the electrical consumption and the capital expenditure thus justifying its installation only in the case of concurrent integration of DISPLACE. On the other hand, oxy-fired units produce exhaust gas streams with higher CO_2 concentrations compared to the conventional equipment, making the CO_2 capture process less energy-intensive. Furthermore, a larger ASU can increase revenues from the sale of argon, partially compensating the higher expenditures. The CASOH process could potentially benefit from the use of oxygen in the blast furnace as well, generating a more concentrated H_2-rich stream, even if this was not explored in this study.

For scenarios where oxy-fired hot stoves or reheating ovens are not adopted, some coke oven gas must be used alongside blast furnace gas to ensure that sufficient thermal energy is transferred to the hot-blast air and slabs. To simulate these conditions, hot stoves and reheating ovens have been modelled in Aspen Plus. In these simulations, air is used as the comburent instead of pure oxygen, with a mixture of BFG and COG as fuel. The mass flow rate of air has been calculated to achieve 1 % oxygen in the exhaust gases. The results of these simulations are presented in Table 13.

The available coke oven gas, which is not already used as fuel within the steel plant, was prioritized as the primary fuel source to meet the additional heat requirements for the DISPLACE CO_2 capture process, while exporting the hydrogen-rich stream from CASOH. If the available COG is insufficient to cover the DISPLACE heat demand, the hydrogen-rich stream is utilized as an additional fuel, with any excess being exported. Conversely, the heat demand of the CASOH process is fulfilled by using part of the H_2-rich mixture as fuel.

Gas distribution within the steel plant when carbon capture process is simultaneously applied to flue gas from hot stoves, reheating ovens and sinter plant, along with pre-combustion CASOH technology is shown in Fig. 6. Table 14 details the amount of COG and H_2-rich mix exported in the analysed cases. For the base and reference BF-BOF cases there is no export of COG or H_2-rich mix.

The breakdown of CO_2 emissions for C^{4}U steel plant, considering

Table 14
Export of COG, H_2-rich mix, Ar for the analysed cases.

Gas exported	CASOH	RO	HS	HS-RO	HS-RO-SP
COG [kg/t_{HRC}]	34.43	31.05	20.07	9.38	-
COG [kg/h]	13270	11964	7734	3616	-
H_2-rich mix [kg/t_{HRC}]	200.06	200.06	200.06	200.06	60.91
H_2-rich mix [kg/h]	77097	77097	77097	77097	23474
Ar [kg/t_{HRC}]	2.88	4.81	5.04	6.98	6.98
Ar [kg/h]	1109	1855	1943	2689	2689

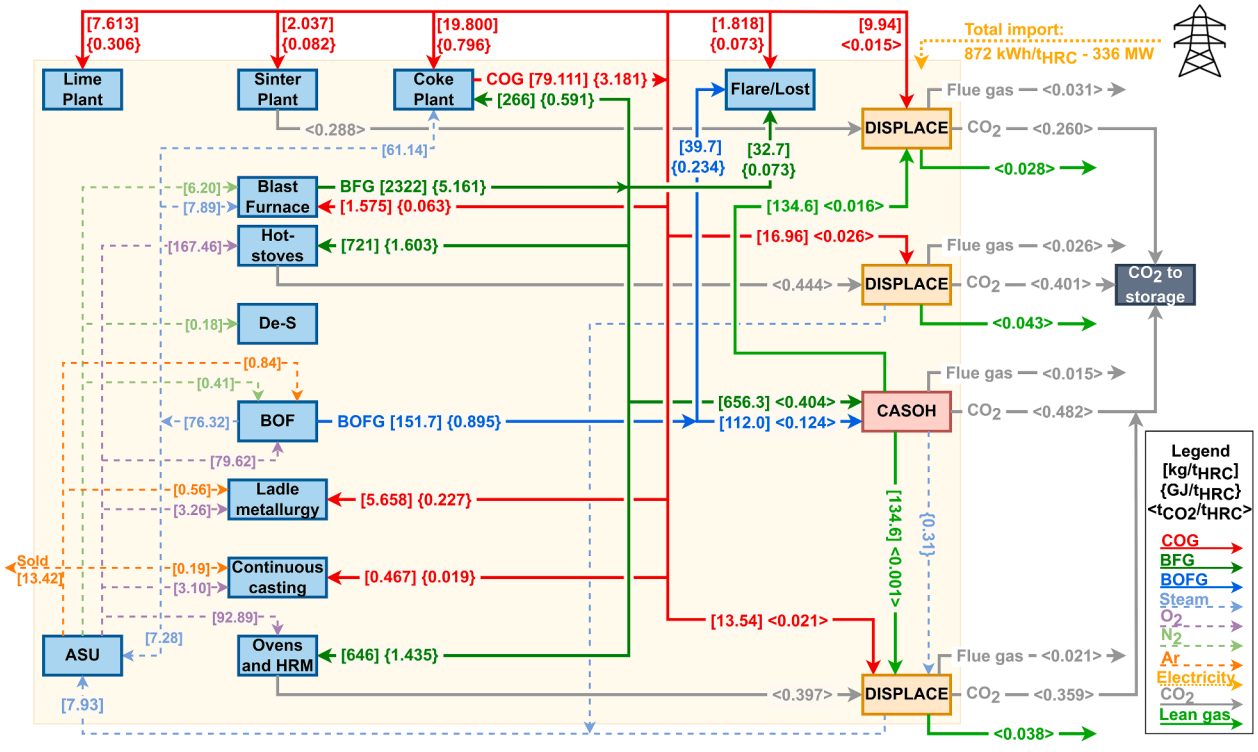

Fig. 6. C^{4}U steel plant layout. Gas distribution within the units.

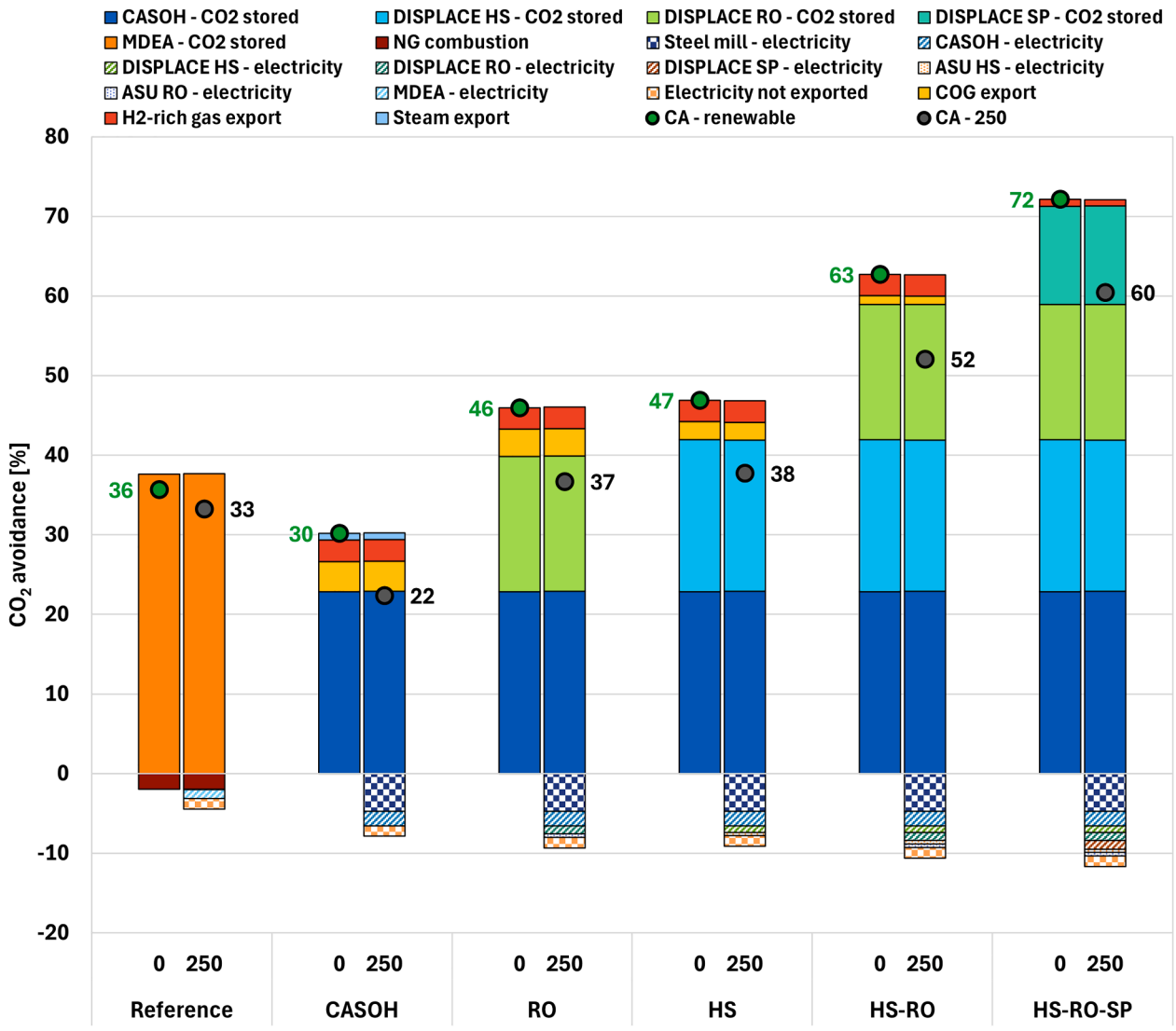

Fig. 7. CO_2 avoidance of C^4U steel mill with respect to base BF-BOF plant when considering different combinations of implementation of DISPLACE and CASOH. The values in green and in black represent the CO_2 avoidance that can be achieved when considering a carbon intensity of imported electricity equal to 0 and 250 kg_{CO2}/MWh_{el} respectively.

various combinations of DISPLACE and CASOH implementation, is summarised in Table B.1. Figure 7 illustrates the CO_2 avoidance computed with respect to the base BF-BOF plant. The values shown in green and black represent the CO_2 avoidance achievable under fully renewable and 250 kg_{CO2}/MWh_{el} electricity scenarios and result from the net sum of positive and negative contributions illustrated in the column chart. In the non-renewable energy scenario, the total CO_2 avoidance is primarily reduced due to indirect emissions associated with electricity imports. For the reference steel plant, additional CO_2 emissions arising from the combustion of natural gas for steam generation further decrease the overall CO_2 avoidance. The resulting CO_2 avoidance, for this case, ranges between 33 % and 36 %, as only the gas streams utilized as fuel in the power plant (a part of BFG and BOFG) are subjected to decarbonization, as previously explained. In contrast, for the C^4U steel mill, the integration of multiple CO_2 capture units significantly enhances the overall CO_2 avoidance. A maximum CO_2 avoidance of 72 % can be achieved under a fully renewable energy scenario when the CASOH system is combined with three DISPLACE units.

Table B.2 presents the breakdown of primary energy consumption for the analysed C^4U steel plant, while Fig. 8 illustrates the SPECCA across different scenarios. The primary energy consumption related to COG and H_2-rich is calculated on the basis of the LHV and these values are negative in case of export from the plant. Interestingly, for the C^4U steel plant, the positive factors of SPECCA are all associated with electricity imported from the grid or to the non-export of electricity. Therefore, in a renewable energy scenario where electricity is produced without fossil fuels consumption, and thus considering 0 GJ_{LHV}/MWh_{el} for the primary energy consumption associated to electricity generation, the SPECCA results being negative. Conversely, in scenarios where fossil fuels contribute to electricity generation, the absence of a power cycle in the C^4U plant significantly influences the SPECCA. The SPECCA related to the power consumption of CASOH is primarily due to the calcination process operating at 0.5 bar to produce nearly pure CO_2, which is subsequently compressed to 110 bar for transportation and storage. The electricity required for CO_2 compression is in fact accounted for in all cases.

Table 15 provides the breakdown of the levelized cost of hot rolled coil, with negative values indicating revenues. Further details are given in Table B.3. The levelized cost of hot rolled coil is 508.5 $€/t_{HRC}$ for the base steel plant. This cost increases as carbon capture technologies are integrated, reaching 718.3 $€/t_{HRC}$ at the highest level of CO_2 avoidance. Fig. 9 displays the cost CO_2 avoided across different scenarios. The electricity not sold increases the CCA for all cases since electricity is imported from the grid differently from the base BF-BOF plant, where

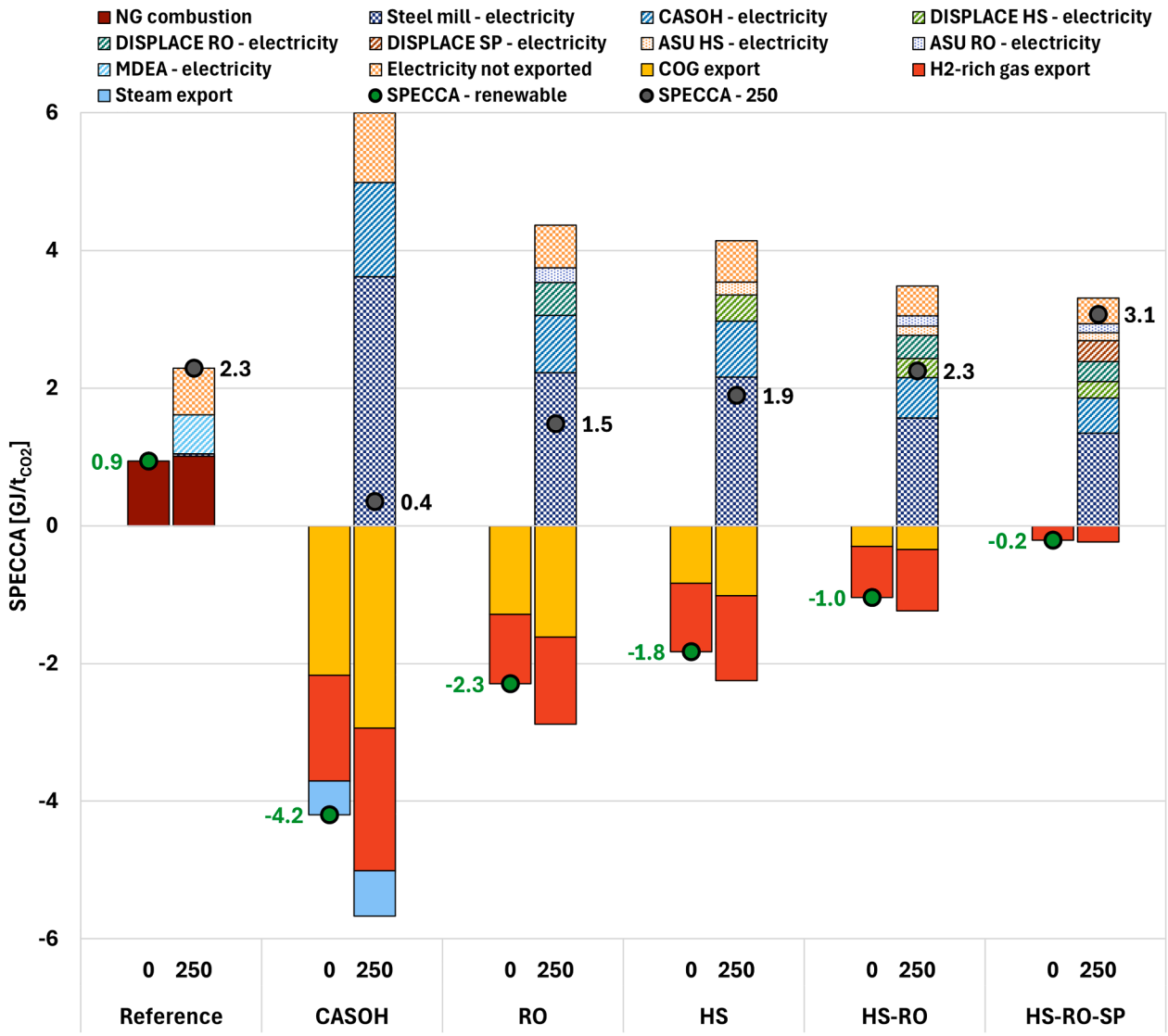

Fig. 8. SPECCA of C^{4}U steel mill with respect to base BF-BOF plant when considering different combinations of implementation of DISPLACE and CASOH. The values in green and in black represent the SPECCA considering a carbon intensity of imported electricity equal to 0 and 250 kg_{CO2}/MWh_{el} respectively.

Table 15
Breakdown of levelized cost of hot rolled coil for the analysed plants. All values are expressed in [€/t_{HRC}].

LCOHRC [€/t_{HRC}]	Base	Ref.	CASOH	RO	HS	HS-RO	HS-RO-SP
CAPEX	118.7	133.6	141.8	151.7	152.3	162.0	170.6
- Steel mill	118.7	117.4	113.0	114.5	114.7	116.1	116.1
- CASOH	-	-	28.8	28.8	28.8	28.8	28.8
- DISPLACE	-	-	-	8.3	8.8	17.1	25.7
- MDEA	-	16.1	-	-	-	-	-
OPEX	406.0	460.7	489.8	519.8	519.0	549.0	570.7
- Electricity	-	12.3	68.9	84.5	82.0	97.7	108.9
- Natural gas	-	9.8	-	-	-	-	-
- Other OPEX	406.0	438.6	421.0	435.3	437.0	451.3	461.8
REVENUES	-16.2	-11.6	-61.1	-56.5	-50.6	-46.3	-23.0
- COG export	-	-	-19.2	-17.3	-11.2	-5.2	-
- H_2-rich mix export	-	-	-26.0	-26.0	-26.0	-26.0	-7.9
- Steam export	-	-	-4.3	-	-	-	-
- Other revenues	-16.2	-11.6	-11.6	-13.2	-13.4	-15.1	-15.1
Total	508.5	582.7	570.5	614.9	620.7	664.7	718.3

electricity is exported and generates revenue. Many factors influence the CCA, including natural gas and electricity prices, as well as the carbon footprint of imported electricity. The carbon footprint of electricity directly impacts CO_2 avoidance and consequently the CCA. This has a bigger impact on the C^{4}U steel mill compared to the reference case, since all the electricity is imported from the grid. In the case of a higher price of natural gas the revenues from the sale of coke oven gas (COG) and hydrogen-nitrogen mixture (H_2-rich) increase, as their prices are linked to natural gas price, decreasing the CCA of the C^{4}U steel mill. The reference and CASOH cases present similar results in the renewable energy scenario, while the cost of CO_2 avoided increases when multiple point sources are decarbonised within the C^{4}U steel mill. In a renewable energy scenario, with a CO_2 avoidance of 72 % the cost of CO_2 avoided is equal to 138 €/t_{CO2}.

Fig. 10 shows the results in the case of availability of electricity at a price of 50 €/MWh_{el}. As can be observed the reference case is less influenced by this parameter while the CCA of C^{4}U stell mill sensibly decreases. In the renewable energy scenario, the CCA of the C^{4}U is equal to 92 €/t_{CO2} with a CO_2 avoidance equal to 72 % while the reference case shows a CCA of 85 €/t_{CO2} with a CO_2 avoidance limited to 36 %.

Furthermore, a sensitivity analysis on CCA was performed varying four key parameters: i) natural gas price, ranging from 25 to 100

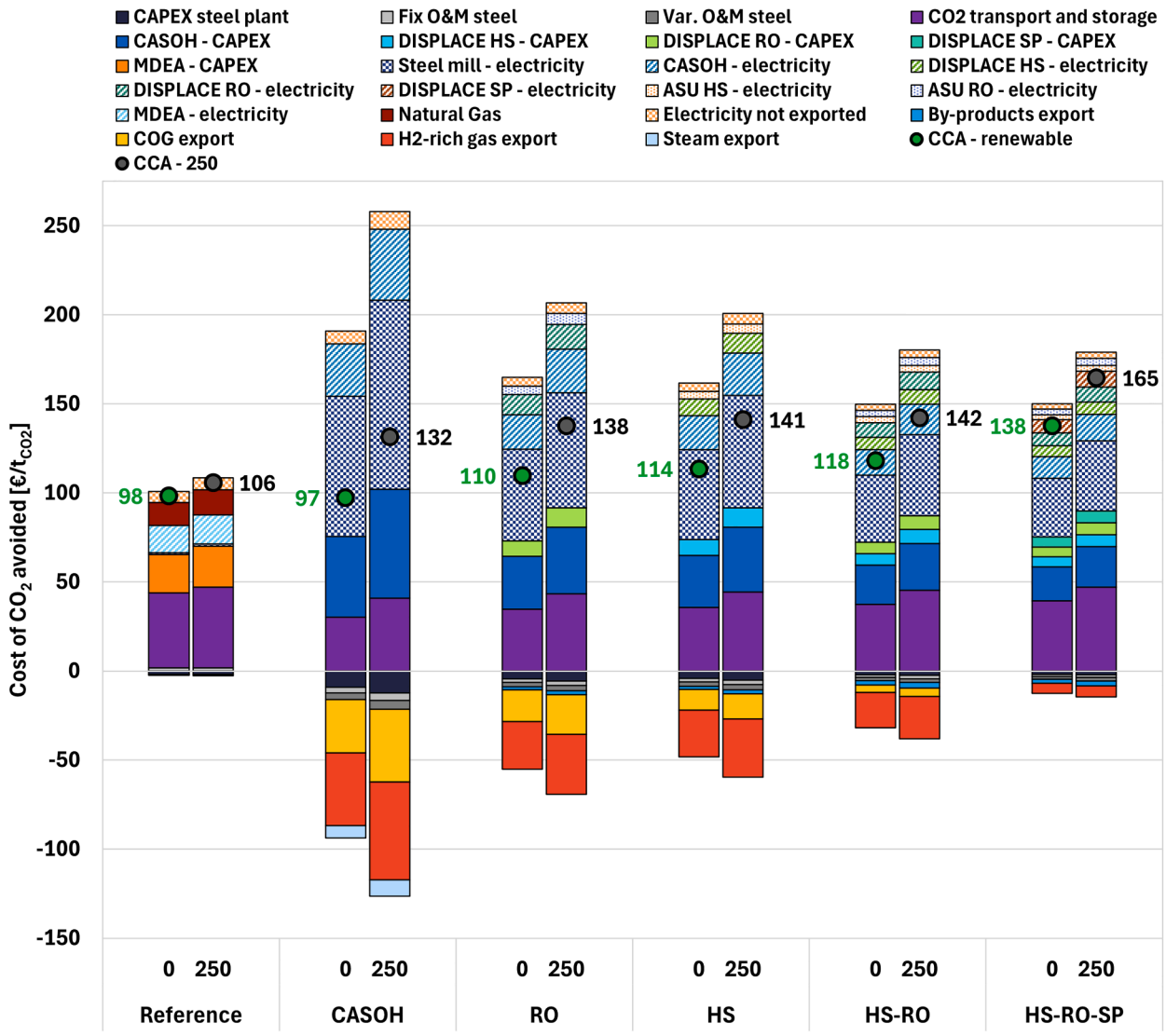

Fig. 9. Cost of CO_2 avoided of C^{4}U steel mill with respect to base BF-BOF plant when considering different combinations of implementation of DISPLACE and CASOH. The values in green and in black represent the CCA considering a carbon intensity of imported electricity equal to 0 and 250 kg_{CO2}/MWh_{el} respectively.

€/MWh, ii) electricity price, varying from 50 to 200 €/MWh, (iii) CO_2 transport and storage cost, ranging from 40 to 140 €/$t_{CO2\ stored}$, iv) CO_2 footprint of electricity imported from the grid, considering a renewable scenario (zero emissions) and a scenario with a footprint of 250 kg_{CO2}/MWh. The results of this analysis are presented in the supplementary material.

4. Conclusions

Among the hard-to-abate sectors, steel industry is one of the major contributors to CO_2 emissions worldwide. In the long term, DRI process using green hydrogen is considered a good option, however, in the short term, alternatives must be explored. These alternative solutions must be integrated in BF-BOF steel plants and be capable of capturing CO_2 from multiple streams with different characteristics in energy content and CO_2 concentration. This work investigates two innovative CO_2 capture technologies developed and demonstrated at TRL 7 in the C^{4}U project, named DISPLACE and CASOH, when integrated in a conventional BF-BOF steel mill to significantly reduce CO_2 emissions. CASOH processes a mixture of BFG and BOFG producing pure hydrogen and a concentrated CO_2 stream, while DISPLACE captures the CO_2 present in the exhaust gases coming from hot stoves, reheating ovens and sinter plant. Detailed analyses were conducted to optimize operational conditions for DISPLACE in various units, revealing its superiority over the benchmark MEA post-combustion technology under certain CO_2 concentration thresholds. Models of CASOH and DISPLACE where integrated in Aspen Plus V14 flowsheet to develop accurate heat and mass balances of the system as well component design for cost assessment. The two technologies, when simultaneously integrated, can achieve a CO_2 avoidance of 72 % and a corresponding SPECCA of -0.2 GJ/t_{CO2} when green electricity is purchased from the grid. In the same scenario, the reference case shows a CO_2 avoidance of 36 % and a SPECCA equal to 0.9 GJ/t_{CO2}. From an economic perspective, the adoption of CO_2 capture technologies increases the cost of HRC to 718.3 €/t_{HRC} which is 41 % higher than the base case (without CO_2 capture), calculated assuming a cost of electricity and NG equal to 125 €/MWh_{el} and 50 €/MWh_{LHV}.

The cost of CO_2 avoided ranges between 138 €/t_{CO2} for the fully green and 165 €/t_{CO2} for electricity with 250 kg_{CO2}/MWh_{el} CO_2 emissions intensity. These values are higher than the corresponding one for the reference CO_2 capture technology considered, however doubling the CO_2 avoidance. It is worth to be underlined that the economic results are highly influenced by the prices of electricity and fuels. The techno-economic analysis, indeed, shows that in a scenario with low prices of electricity (i.e. 50 €/MWh_{el}), the cost of CO_2 avoided of the C^{4}U steel

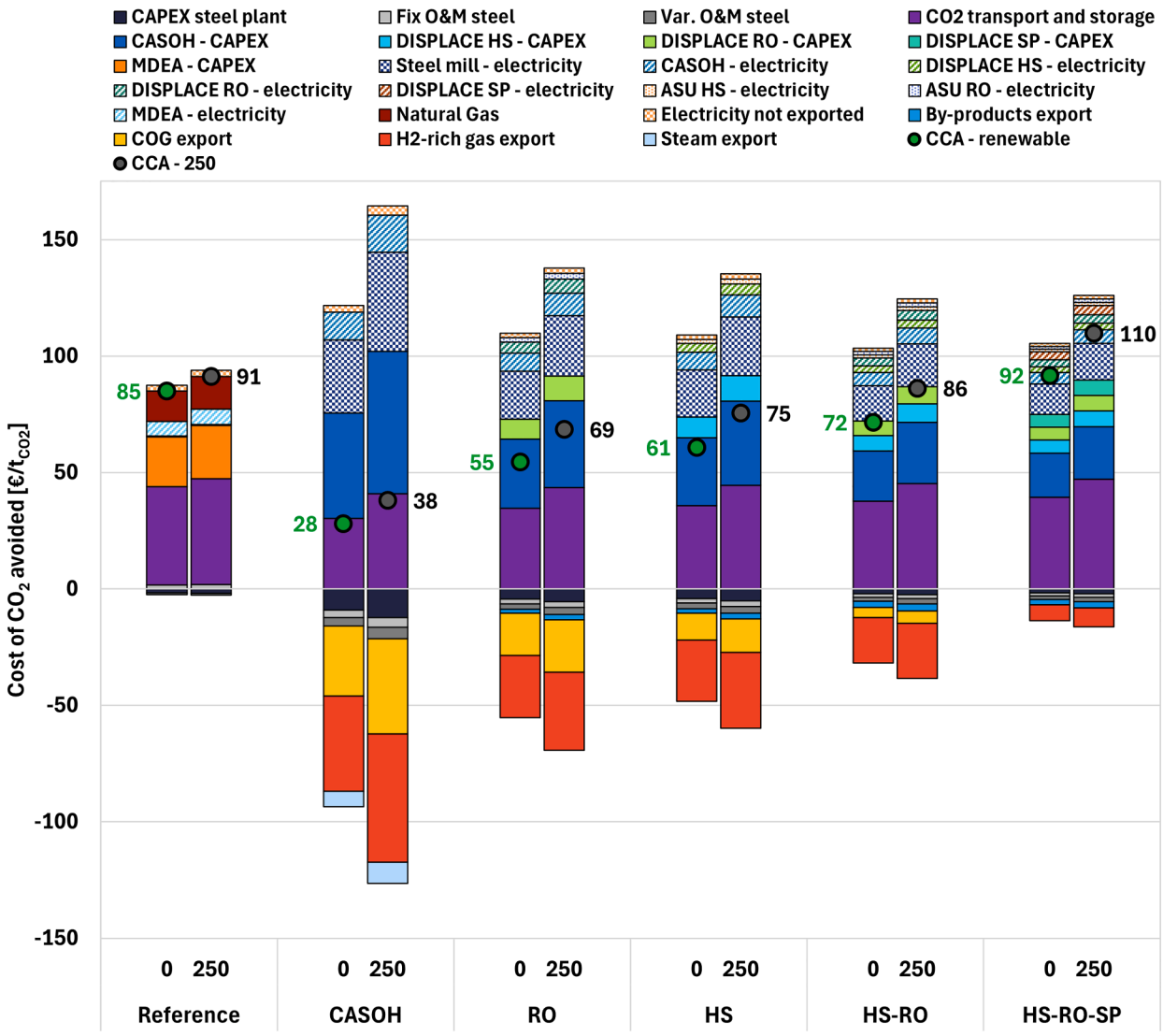

Fig. 10. Cost of CO_2 avoided of C^{4}U steel mill with respect to base BF-BOF plant when considering different combinations of implementation of DISPLACE and CASOH. The values in green and in black represent the CCA considering a carbon intensity of imported electricity equal to 0 and 250 kg_{CO2}/MWh_{el} respectively. Electricity and natural gas prices set to 50 €/MWh_{el} and 50 €/MWh_{LHV}.

mill reduces to 92 €/t_{CO2} in the case of renewable electricity, becoming closer to the CCA of the reference case. A sensitivity analysis regarding key parameters influencing the outcomes of the techno-economic analysis is included in the supplementary material. Further studies will investigate the utilization of H_2 with CO_2 for production of chemicals such as methanol and addressing additional flue gases as the one from lime plant to further increase the CO_2 avoided.

CRediT authorship contribution statement

Nicola Zecca: Writing – original draft, Visualization, Validation, Software, Methodology, Investigation, Formal analysis, Data curation, Conceptualization. **Santiago Zapata Boada:** Writing – review & editing, Software, Methodology, Investigation, Formal analysis, Data curation, Conceptualization. **Vincenzo Spallina:** Writing – review & editing, Supervision, Methodology, Funding acquisition, Conceptualization. **Giampaolo Manzolini:** Writing – review & editing, Supervision, Project administration, Methodology, Funding acquisition, Conceptualization.

Declaration of competing interest

The authors declare the following financial interests/personal relationships which may be considered as potential competing interests:

Nicola Zecca reports financial support was provided by EU Framework Programme for Research and Innovation Societal Challenges. If there are other authors, they declare that they have no known competing financial interests or personal relationships that could have appeared to influence the work reported in this paper.

Acknowledgements

This paper is part of the C^{4}U project that has received funding from the European Union's Horizon 2020 research and innovation programme under grant agreement N 884418.

The work reflects only the authors' views, and the European Union is not liable for any use that may be made of the information contained therein.

Supplementary materials

Supplementary material associated with this article can be found, in the online version, at doi:10.1016/j.ijggc.2025.104478.

Appendix A

In Table A.1 the specifications of the streams indicated in Fig. 4 referring to the 5 bar – 400°C case are given. Table A.2 lists the specifications of the streams shown in Fig. 5.

Table A.1
Main streams specifications of DISPLACE plant integration. Case 5 bar – 400°C.

Stream	Temperature [°C]	Pressure [bar]	Mass flow rate [kg/s]	Composition [%mol]									
				H_2O	H_2	CO	CO_2	N_2	O_2	CH_4	C_2H_6	C_3H_8	C_5H_{12}
1	500.0	1.2	78.6	6.2	-	-	41.9	50.8	1.0	-	-	-	-
2	277.3	1.0	78.6	6.2	-	-	41.9	50.8	1.0	-	-	-	-
3	167.5	0.8	78.6	6.2	-	-	41.9	50.8	1.0	-	-	-	-
4	157.1	0.6	78.6	6.2	-	-	41.9	50.8	1.0	-	-	-	-
5	35.0	0.4	78.6	6.2	-	-	41.9	50.8	1.0	-	-	-	-
6	191.6	5.2	78.6	6.2	-	-	41.9	50.8	1.0	-	-	-	-
7	400.0	5.0	78.6	6.2	-	-	41.9	50.8	1.0	-	-	-	-
8	395.7	4.8	71.1	61.1	-	-	2.7	35.5	0.7	-	-	-	-
9	127.6	4.0	71.1	61.1	-	-	2.7	35.5	0.7	-	-	-	-
10	400.0	4.8	45.8	26.0	-	-	70.6	3.3	-	-	-	-	-
11	34.9	110.0	38.8	0.3	-	-	95.3	4.4	-	-	-	-	-
12	20.0	1.2	1.4	3.2	60.1	-	1.0	5.8	-	23.2	2.7	-	-
13	15.0	1.0	22.1	-	-	-	-	79.0	21.0	-	-	-	-
14	100.0	1.0	23.5	20.5	0.1	0.1	5.7	70.2	3.0	-	-	-	-
15	15.0	1.0	38.8	100.0	-	-	-	-	-	-	-	-	-
16	102.0	1.3	4.7	100.0	-	-	-	-	-	-	-	-	-
17	102.0	1.3	26.4	100.0	-	-	-	-	-	-	-	-	-
18	102.0	1.3	7.7	100.0	-	-	-	-	-	-	-	-	-
19	102.0	7.2	39.2	100.0	-	-	-	-	-	-	-	-	-
20	107.2	5.8	5.9	100.0	-	-	-	-	-	-	-	-	-
21	157.5	5.8	4.3	100.0	-	-	-	-	-	-	-	-	-
22	157.5	5.8	11.8	100.0	-	-	-	-	-	-	-	-	-
23	157.5	5.8	16.7	100.0	-	-	-	-	-	-	-	-	-
24	400.0	5.4	38.3	100.0	-	-	-	-	-	-	-	-	-
25	152.9	4.5	0.5	100.0	-	-	-	-	-	-	-	-	-

Table A.2
Main streams specifications of the CASOH process.

Stream	Temperature[°C]	Pressure[bar]	Mass flow rate[kg/s]	Composition [%mol]					
				H_2O	H_2	CO	CO_2	N_2	O_2
1	35.5	1.1	81.8	4.4	2.4	27.4	19.8	46.0	-
2	517.7	9.7	106.9	36.8	1.6	18.2	13.1	30.4	-
3	749.5	9.2	55.2	27.6	26.1	1.6	2.2	42.6	-
4	210.0	9.2	55.2	27.6	26.1	1.6	2.2	42.6	-
5	525.0	8.5	8.3	27.6	26.1	1.6	2.2	42.6	-
6	676.0	8.0	10.3	53.3	-	-	3.7	42.3	0.6
7	210.0	8.0	10.3	53.3	-	-	3.7	42.3	0.6
8	35.0	8.0	6.1	0.6	-	-	7.9	90.1	1.4
9	30.0	8.2	34.7	0.5	35.8	2.1	3.0	58.6	-
10	25.0	1.0	35.8	100.0	-	-	-	-	-
11	525.0	2.8	9.0	100.0	-	-	-	-	-
12	832.8	0.5	60.6	29.8	-	-	70.2	-	-
13	210.0	0.5	60.6	29.8	-	-	70.2	-	-
14	38.3	110.0	51.8	0.6	-	-	99.4	-	-
15	25.0	1.0	8.7	-	-	-	-	79.0	21.0
16	190.5	10.6	8.7	-	-	-	-	79.0	21.0
17	601.9	9.0	6.7	-	-	-	-	100.0	-
18	210.0	9.0	6.7	-	-	-	-	100.0	-
19	15.0	1.1	1.0	-	-	-	-	100.0	-
20	192.4	9.5	1.0	-	-	-	-	100.0	-
21	602.0	9.5	1.0	-	-	-	-	100.0	-
22	210.0	9.5	1.0	-	-	-	-	100.0	-
23	132.2	1.0	13.8	0.3	-	-	3.4	95.7	0.6

Appendix B

In this section, the detailed results of the analysed plants, specifically the breakdown of CO_2 emissions (Table B.1), of primary energy consumption (Table B.2) and of the levelized cost of hot rolled coil (Table B.3) are given.

Table B.1
Breakdown of CO_2 emissions for C^{4}U steel plants. All values are expressed in [t_{CO2}/t_{HRC}] and negative values indicate CO_2 stored or related to fuel export. The results refer to the scenario in which the carbon intensity of electricity imported from the grid has a carbon footprint equal to 250 $kg_{CO2}/MWh_{el.}$

CO_2 emission [t_{CO2}/t_{HRC}]	Base	Ref.	CASOH	RO	HS	HS-RO	HS-RO-SP
Iron ore production	0.067	0.067	0.067	0.067	0.067	0.067	0.067
CO_2 in steel mill	2.068	2.068	2.068	2.068	2.068	2.068	2.068
CO_2 not treated	-	1.109	1.541	1.144	1.097	0.700	0.412
CO_2 treated	-	0.959	0.527	0.924	0.971	1.368	1.656
CO_2 to storage	-	-0.794	-0.482	-0.841	-0.883	-1.242	-1.502
- CASOH	-	-	-0.482	-0.482	-0.482	-0.482	-0.482
- DISPLACE HS	-	-	-	-	-0.401	-0.401	-0.401
- DISPLACE RO	-	-	-	-0.359	-	-0.359	-0.359
- DISPLACE SP	-	-	-	-	-	-	-0.260
- MDEA	-	-0.794	-	-	-	-	-
Lean streams	-	0.165	0.045	0.083	0.088	0.126	0.154
- CASOH	-	-	0.045	0.045	0.045	0.045	0.045
- DISPLACE HS	-	-	-	-	0.043	0.043	0.043
- DISPLACE RO	-	-	-	0.038	-	0.038	0.038
- DISPLACE SP	-	-	-	-	-	-	0.028
- MDEA	-	0.165	-	-	-	-	-
NG combustion	-	0.041	-	-	-	-	-
Electricity import	-	0.025	0.138	0.169	0.164	0.195	0.218
- Steel mill	-	0.001	0.100	0.100	0.100	0.100	0.100
- CASOH	-	-	0.038	0.038	0.038	0.038	0.038
- DISPLACE HS	-	-	-	-	0.018	0.018	0.018
- DISPLACE RO	-	-	-	0.022	-	0.022	0.022
- DISPLACE SP	-	-	-	-	-	-	0.023
- ASU for HS	-	-	-	-	0.009	0.009	0.009
- ASU for RO	-	-	-	0.010	-	0.010	0.010
- MDEA	-	0.023	-	-	-	-	-
Electricity export	-0.028	-	-	-	-	-	-
COG export	-	-	-0.080	-0.072	-0.047	-0.022	-
H_2-rich mix export	-	-	-0.057	-0.057	-0.057	-0.057	-0.017
Steam export	-	-	-0.018	-	-	-	-
Total	2.107	1.406	1.636	1.334	1.313	1.010	0.834

Table B.2
Breakdown of primary energy consumption for C^{4}U steel plants. All values are expressed in [GJ/t_{HRC}]. The results refer to the scenario in which the carbon intensity of electricity imported from the grid has a carbon footprint equal to 250 kg_{CO2}/MWh_{el}.

PEC [GJ/t_{HRC}]	Base	Ref.	CASOH	RO	HS	HS-RO	HS-RO-SP
Cocking coal	16.41	16.41	16.41	16.41	16.41	16.41	16.41
PCI coal	5.32	5.32	5.32	5.32	5.32	5.32	5.32
Natural gas	-	0.71	-	-	-	-	-
Electricity	-	0.42	2.36	2.90	2.81	3.35	3.74
- Steel mill	-	0.02	1.72	1.72	1.72	1.72	1.72
- CASOH	-	-	0.64	0.64	0.64	0.64	0.64
- DISPLACE HS	-	-	-	-	0.30	0.30	0.30
- DISPLACE RO	-	-	-	0.37	-	0.37	0.37
- DISPLACE SP	-	-	-	-	-	-	0.39
- ASU for HS	-	-	-	-	0.15	0.15	0.15
- ASU for RO	-	-	-	0.16	-	0.16	0.16
- MDEA	-	0.40	-	-	-	-	-
Electricity export	-0.48	-	-	-	-	-	-
COG export	-	-	-1.38	-1.25	-0.81	-0.38	-
H_2-rich mix export	-	-	-0.98	-0.98	-0.98	-0.98	-0.30
Steam export	-	-	-0.31	-	-	-	-
Total	21.25	22.86	21.42	22.40	22.76	23.72	25.17

Table B.3
Breakdown of levelized cost of hot rolled coil for C^{4}U steel plants. All values are expressed in [€/t_{HRC}]. The results refer to the scenario in which electricity and natural gas prices are equal to 125 €/MWh_e and 50 €/MWh_{LHV} respectively.

LCOHRC [€/t_{HRC}]	Base	Ref.	CASOH	RO	HS	HS-RO	HS-RO-SP
CAPEX steel mill	118.7	117.4	113.0	114.5	114.7	116.1	116.1
Fix. O&M steel mill	99.1	100.5	97.1	97.1	97.1	97.1	97.1
Var. O&M steel mill	290.7	290.2	288.4	288.4	288.4	288.4	288.4
Misc. OPEX steel mill	14.3	14.3	14.3	14.3	14.3	14.3	14.3
Other O&M costs steel mill	1.8	1.8	1.8	1.8	1.8	1.8	1.8
CO_2 transport and storage	-	31.8	19.3	33.6	35.3	49.7	60.1
CAPEX CASOH	-	-	28.8	28.8	28.8	28.8	28.8
CAPEX DISPLACE HS	-	-	-	-	8.8	8.8	8.8
CAPEX DISPLACE RO	-	-	-	8.3	-	8.3	8.3
CAPEX DISPLACE SP	-	-	-	-	-	-	8.5
CAPEX MDEA	-	16.1	-	-	-	-	-
Electricity import steel mill	-	0.7	50.1	50.1	50.1	50.1	50.1
Electricity import CASOH	-	-	18.8	18.8	18.8	18.8	18.8
Electricity import DISPLACE HS	-	-	-	-	8.8	8.8	8.8
Electricity import DISPLACE RO	-	-	-	10.8	-	10.8	10.8
Electricity import DISPLACE SP	-	-	-	-	-	-	11.3
Electricity import ASU for HS	-	-	-	-	4.3	4.3	4.3
Electricity import ASU for RO	-	-	-	4.8	-	4.8	4.8
Electricity import MDEA	-	11.6	-	-	-	-	-
Electricity export	-4.6	-	-	-	-	-	-
Natural gas	-	9.8	-	-	-	-	-
Other revenues	-11.6	-11.6	-11.6	-13.2	-13.4	-15.1	-15.1
COG export	-	-	-19.2	-17.3	-11.2	-5.2	-
H_2-rich mix export	-	-	-26.0	-26.0	-26.0	-26.0	-7.9
Steam export	-	-	-4.3	-	-	-	-
Total	508.5	582.7	570.5	614.9	620.7	664.7	718.3

Data availability

Data will be made available on request.

References

Abanades, J.C., Murillo, R., Fernandez, J.R., Grasa, G., Martínez, I., 2010. New CO2 capture process for hydrogen production combining Ca and Cu chemical loops. Env. Sci. Technol 44, 6901–6904. https://doi.org/10.1021/es101707t.

Abbas, S.Z., Argyris, P.A., Fernández, J.-R., Abanades, J.C., Spallina, V., 2021. A Ca-Cu chemical loop process for CO2 capture in steel mills: system performance analysis. In: Proceedings of the 15th Greenhouse Gas Control Technologies Conference 15-18 March 2021.

Abbas, S.Z., Fernández, J.R., Amieiro, A., Rastogi, M., Brandt, J., Spallina, V., 2022. Lab-scale experimental demonstration of CaCu chemical looping for hydrogen production and in-situ CO2 capture from a steel-mill. Fuel Process. Technol. 237, 107475. https://doi.org/10.1016/j.fuproc.2022.107475.

Abdul Quader, M., Ahmed, S., Dawal, S.Z., Nukman, Y., 2016. Present needs, recent progress and future trends of energy-efficient Ultra-low carbon dioxide (CO2) steelmaking (ULCOS) program. Renew. Sustain. Energy Rev. 55, 537–549. https://doi.org/10.1016/j.rser.2015.10.101.

Antonini, C., Pérez-Calvo, J.-F., van der Spek, M., Mazzotti, M., 2021. Optimal design of an MDEA CO2 capture plant for low-carbon hydrogen production — A rigorous process optimization approach. Sep. Purif. Technol 279, 119715. https://doi.org/10.1016/j.seppur.2021.119715.

Arasto, A., Tsupari, E., Kärki, J., Lilja, J., Sihvonen, M., 2014. Oxygen blast furnace with CO2 capture and storage at an integrated steel mill—Part I: technical concept analysis. Int. J. Greenh. Gas Control 30, 140–147. https://doi.org/10.1016/j.ijggc.2014.09.004.

Arasto, A., Tsupari, E., Kärki, J., Pisilä, E., Sorsamäki, L., 2013a. Post-combustion capture of CO2 at an integrated steel mill - part I: technical concept analysis. Int. J. Greenh. Gas Control 16, 271–277. https://doi.org/10.1016/j.ijggc.2012.08.018.

Arasto, A., Tsupari, E., Kärki, J., Sihvonen, M., Lilja, J., 2013b. Costs and potential of carbon capture and storage at an integrated steel mill. Energy Procedia 37, 7117–7124. https://doi.org/10.1016/j.egypro.2013.06.648.

Arias, B., Diego, M.E., Abanades, J.C., Lorenzo, M., Diaz, L., Martínez, D., Alvarez, J., Sánchez-Biezma, A., 2013. Demonstration of steady state CO2 capture in a 1.7MWth calcium looping pilot. Int. J. Greenh. Gas Control 18, 237–245. https://doi.org/10.1016/j.ijggc.2013.07.014.

Astolfi, M., De Lena, E., Casella, F., Romano, M.C., 2021. Calcium looping for power generation with CO2 capture: the potential of sorbent storage for improved economic performance and flexibility. Appl. Therm. Eng 194, 117048. https://doi.org/10.1016/j.applthermaleng.2021.117048.

Baker, R.W., Freeman, B., Kniep, J., Huang, Y.I., Merkel, T.C., 2018. CO2 Capture from cement plants and steel mills using membranes. Ind. Eng. Chem. Res 57, 15963–15970. https://doi.org/10.1021/acs.iecr.8b02574.

Biermann, M., Ali, H., Sundqvist, M., Larsson, M., Normann, F., Johnsson, F., 2019. Excess heat-driven carbon capture at an integrated steel mill – Considerations for capture cost optimization. Int. J. Greenh. Gas Control 91, 102833. https://doi.org/10.1016/j.ijggc.2019.102833.

Birat, J.-P., 2010. 16 - Carbon dioxide (CO2) capture and storage technology in the iron and steel industry. In: Maroto-Valer, M.M. (Ed.), Developments and Innovation in Carbon Dioxide (CO2) Capture and Storage Technology. Woodhead Publishing, pp. 492–521. https://doi.org/10.1533/9781845699574.5.492.

C4U website [WWW Document], n.d. URL https://c4u-project.eu/(accessed 11.12.24).

Chamchan, N., Chang, J.-Y., Hsu, H.-C., Kang, J.-L., Wong, D.S.H., Jang, S.-S., Shen, J.-F., 2017. Comparison of rotating packed bed and packed bed absorber in pilot plant and model simulation for CO2 capture. J. Taiwan. Inst. Chem. Eng 73, 20–26. https://doi.org/10.1016/j.jtice.2016.08.046.

Cheng, H.-H., Shen, J.-F., Tan, C.-S., 2010. CO2 capture from hot stove gas in steel making process. Int. J. Greenh. Gas Control 4, 525–531. https://doi.org/10.1016/j.ijggc.2009.12.006.

Chisalita, D.-A., Petrescu, L., Cobden, P., van Dijk, H.A.J.(Eric), Cormos, A.-M., Cormos, C.-C., 2019. Assessing the environmental impact of an integrated steel mill with post-combustion CO2 capture and storage using the LCA methodology. J. Clean. Prod 211, 1015–1025. https://doi.org/10.1016/j.jclepro.2018.11.256.

Chung, W., Roh, K., Lee, J.H., 2018a. Design and evaluation of CO2 capture plants for the steelmaking industry by means of amine scrubbing and membrane separation. Int. J. Greenh. Gas Control 74, 259–270. https://doi.org/10.1016/j.ijggc.2018.05.009.

Chung, W., Roh, K., Lee, J.H., 2018b. Design and evaluation of CO2 capture plants for the steelmaking industry by means of amine scrubbing and membrane separation. Int. J. Greenh. Gas Control 74, 259–270. https://doi.org/10.1016/j.ijggc.2018.05.009.

Cormos, A.-M., Dragan, S., Petrescu, L., Sandu, V., Cormos, C.-C., 2020a. Techno-economic and environmental evaluations of decarbonized fossil-intensive industrial processes by reactive absorption & adsorption CO2 capture systems. Energ. (Basel) 13. https://doi.org/10.3390/en13051268.

Cormos, A.-M., Dumbrava, I., Cormos, C.-C., 2020b. Evaluation of techno-economic performance for decarbonized hydrogen and power generation based on glycerol thermo-chemical looping cycles. Appl. Therm. Eng 179, 115728. https://doi.org/10.1016/j.applthermaleng.2020.115728.

Cormos, C.-C., 2016. Evaluation of reactive absorption and adsorption systems for post-combustion CO2 capture applied to iron and steel industry. Appl. Therm. Eng 105, 56–64. https://doi.org/10.1016/j.applthermaleng.2016.05.149.

Danloy, G., Berthelemot, A., Grant, M., Borlée, J., Sert, D., van der Stel, J., Jak, H., Dimastromatteo, V., Hallin, M., Eklund, N., Edberg, N., Sundqvist, L., Sköld, B.-E., Lin, R., Feiterna, A., Korthas, B., Müller, F., Feilmayr, C., Habermann, A., 2009. ULCOS - pilot testing of the low-CO2 blast furnace process at the experimental BF in Luleå. Rev. Met. Paris 106, 1–8. https://doi.org/10.1051/metal/2009008.

Fernández, J.R., Martínez, I., Abanades, J.C., Romano, M.C., 2017. Conceptual design of a Ca–Cu chemical looping process for hydrogen production in integrated steelworks.

Int. J. Hydrog. Energy 42, 11023–11037. https://doi.org/10.1016/j.ijhydene.2017.02.141.
Fernández, J.R., Spallina, V., Abanades, J.C., 2020. Advanced packed-bed Ca-Cu looping process for the CO2 capture from steel mill off-gases. Front. Energy Res 8. https://doi.org/10.3389/fenrg.2020.00146.
Gazzani, M., Romano, M.C., Manzolini, G., 2015. CO2 capture in integrated steelworks by commercial-ready technologies and SEWGS process. Int. J. Greenh. Gas Control 41, 249–267. https://doi.org/10.1016/j.ijggc.2015.07.012.
Gentile, G., Bonalumi, D., Pieterse, J.A.Z., Sebastiani, F., Lucking, L., Manzolini, G., 2022. Techno-economic assessment of the FReSMe technology for CO2 emissions mitigation and methanol production from steel plants. J. CO2 Util. 56. https://doi.org/10.1016/j.jcou.2021.101852.
Goto, K., Okabe, H., Chowdhury, F.A., Shimizu, S., Fujioka, Y., Onoda, M., 2011. Development of novel absorbents for CO2 capture from blast furnace gas. Int. J. Greenh. Gas Control 5, 1214–1219. https://doi.org/10.1016/j.ijggc.2011.06.006.
Grasa, G., Díaz, M., Fernández, J.R., Amieiro, A., Brandt, J., Abanades, J.C., 2023. Blast furnace gas decarbonisation through Calcium assisted Steel-mill off-gas hydrogen production. Experimental and modelling approach. Chem. Eng. Res. Des. 191, 507–522. https://doi.org/10.1016/j.cherd.2023.01.047.
Guo, Z., Wang, Q., Fang, M., Luo, Z., Cen, K., 2014. Thermodynamic and economic analysis of polygeneration system integrating atmospheric pressure coal pyrolysis technology with circulating fluidized bed power plant. Appl. Energy 113, 1301–1314. https://doi.org/10.1016/j.apenergy.2013.08.086.
Halmann, M., Steinfeld, A., 2015. Reforming of blast furnace gas with methane, steam, and lime for Syngas production and CO2 capture: A thermodynamic study. Miner. Process. Extr. Metall. Rev. 36, 7–12. https://doi.org/10.1080/08827508.2013.793682.
Hasan, M.M.F., Baliban, R.C., Elia, J.A., Floudas, C.A., 2012. Modeling, simulation, and optimization of postcombustion CO2 capture for variable feed concentration and flow rate. 1. Chemical absorption and membrane processes. Ind. Eng. Chem. Res 51, 15642–15664. https://doi.org/10.1021/ie301571d.
Ho, M.T., Allinson, G.W., Wiley, D.E., 2011. Comparison of MEA capture cost for low CO2 emissions sources in Australia. Int. J. Greenh. Gas Control 5, 49–60. https://doi.org/10.1016/j.ijggc.2010.06.004.
Ho, M.T., Bustamante, A., Wiley, D.E., 2013. Comparison of CO2 capture economics for iron and steel mills. Int. J. Greenh. Gas Control 19, 145–159. https://doi.org/10.1016/j.ijggc.2013.08.003.
Huijgen, W.J.J., Comans, R.N.J., Witkamp, G.-J., 2007. Cost evaluation of CO2 sequestration by aqueous mineral carbonation. Energy Convers. Manage 48, 1923–1935. https://doi.org/10.1016/j.enconman.2007.01.035.
IEAGHG Technical Report, 2013. Iron and steel CCS study (Techno-economics integrated steel mill).
International Energy Agency, 2020. Iron and Steel Technology Roadmap towards more sustainable steelmaking part of the Energy Technology Perspectives series.
International industrial energy prices - GOV.UK [WWW Document], n.d. URL https://www.gov.uk/government/statistical-data-sets/international-industrial-energy-prices (accessed 4.10.24).
Jeon, J.-Y., Park, B.-R., Kim, J.-H., 2022. Numerical simulation and optimization of 4-component LDG separation in the steelmaking industry using polysulfone hollow Fiber membranes. Membr. (Basel) 12. https://doi.org/10.3390/membranes12010097.
Jin, P., Jiang, Z., Bao, C., Hao, S., Zhang, X., 2017. The energy consumption and carbon emission of the integrated steel mill with oxygen blast furnace. Resour. Conserv. Recycl 117, 58–65. https://doi.org/10.1016/j.resconrec.2015.07.008.
Jin, P., Jiang, Z., Bao, C., Lu, Y., Zhang, J., Zhang, X., 2016. Mathematical modeling of the energy consumption and carbon emission for the oxygen blast furnace with top gas recycling. Steel. Res. Int 87, 320–329. https://doi.org/10.1002/srin.201500054.
Katayama, K., Bahzad, H., Boot-Handford, M., Patzschke, C.F., Fennell, P.S., 2020. Process integration of chemical looping water splitting with a sintering plant for iron making. Ind. Eng. Chem. Res 59, 7021–7032. https://doi.org/10.1021/acs.iecr.9b05945.
Khallaghi, N., Abbas, S.Z., Manzolini, G., De Coninck, E., Spallina, V., 2022. Techno-economic assessment of blast furnace gas pre-combustion decarbonisation integrated with the power generation. Energy Convers. Manage 255. https://doi.org/10.1016/j.enconman.2022.115252.
Kim, H., Lee, J., Lee, S., Lee, I.-B., Park, J., Han, J., 2015. Economic process design for separation of CO2 from the off-gas in ironmaking and steelmaking plants. Energy 88, 756–764. https://doi.org/10.1016/j.energy.2015.05.093.
Lewis, E., McNaul, S., Jamieson, M., Henriksen, M.S., Matthews, H.S., Walsh, L., Grove, J., Shultz, T., Skone, T.J., Stevens, R., 2022. Comparison of Commercial, State-of-the-Art. Fossil-Based Hydrogen Production Technologies, United States. https://doi.org/10.2172/1862910.
Li, R., Lian, S., Zhang, Z., Song, C., Han, R., Liu, Q., 2022. Techno-economic evaluation of a novel membrane-cryogenic hybrid process for carbon capture. Appl. Therm. Eng 200, 117688. https://doi.org/10.1016/j.applthermaleng.2021.117688.
Li, Z., Yi, Q., Zhang, Y., Zhou, H., Zhao, Y., Huang, Y., Gao, D., Hao, Y., 2020. Numerical study and design strategy for a low emission coke oven system using oxy-fuel combustion of coke oven gas. J. Clean. Prod 252, 119656. https://doi.org/10.1016/j.jclepro.2019.119656.
Luca, A.-V., Petrescu, L., 2021. Membrane technology applied to steel production: investigation based on process modelling and environmental tools. J. Clean. Prod 294, 126256. https://doi.org/10.1016/j.jclepro.2021.126256.
Luo, M., Wang, C., Yi, Y., Liu, K., Cai, J., Wang, Q., 2018. Power generation from Coke oven gas using chemical looping combustion: thermodynamic simulation. Chem. Eng. Technol 41, 524–531. https://doi.org/10.1002/ceat.201700322.
Manzolini, G., Giuffrida, A., Cobden, P.D., van Dijk, H.A.J., Ruggeri, F., Consonni, F., 2020. Techno-economic assessment of SEWGS technology when applied to integrated steel-plant for CO2 emission mitigation. Int. J. Greenh. Gas Control 94. https://doi.org/10.1016/j.ijggc.2019.102935.
Manzolini, G., Giuffrida, A., Zecca, N., Lücking, L., Pieterse, J.A.Z., Sebastiani, F., Van Dijk, E., 2022. DISPLACE technology to efficiently decarbonize steel industry. In: Proceedings of the 16th Greenhouse Gas Control Technologies Conference (GHGT-16).
Martinez Castilla, G., Biermann, M., Montañés, R.M., Normann, F., Johnsson, F., 2019. Integrating carbon capture into an industrial combined-heat-and-power plant: performance with hourly and seasonal load changes. Int. J. Greenh. Gas Control 82, 192–203. https://doi.org/10.1016/j.ijggc.2019.01.015.
Martínez, I., Fernández, J.R., Abanades, J.C., Romano, M.C., 2018a. Integration of a fluidised bed Ca–Cu chemical looping process in a steel mill. Energy 163, 570–584. https://doi.org/10.1016/j.energy.2018.08.123.
Martínez, I., Fernández, J.R., Abanades, J.C., Romano, M.C., 2018b. Integration of a fluidised bed Ca–Cu chemical looping process in a steel mill. Energy 163, 570–584. https://doi.org/10.1016/j.energy.2018.08.123.
Martínez, I., Fernández, J.R., Martini, M., Gallucci, F., van Sint Annaland, M., Romano, M.C., Abanades, J.C., 2019. Recent progress of the Ca-Cu technology for decarbonisation of power plants and carbon intensive industries. Int. J. Greenh. Gas Control 85, 71–85. https://doi.org/10.1016/j.ijggc.2019.03.026.
Masoudi Soltani, S., Lahiri, A., Bahzad, H., Clough, P., Gorbounov, M., Yan, Y., 2021. Sorption-enhanced steam methane reforming for combined CO2 capture and hydrogen production: A State-of-the-art review. Carbon Capture Sci. Technol. 1, 100003. https://doi.org/10.1016/j.ccst.2021.100003.
Mudhasakul, S., Ku, H., Douglas, P.L., 2013. A simulation model of a CO2 absorption process with methyldiethanolamine solvent and piperazine as an activator. Int. J. Greenh. Gas Control 15, 134–141. https://doi.org/10.1016/j.ijggc.2013.01.023.
Niel, J., Weiss, B., Wukovits, W., 2022. Model of an iron ore sinter plant with selective waste gas recirculation. Carbon Resour. Convers. 5, 71–83. https://doi.org/10.1016/j.crcon.2022.01.001.
Oko, E., Zacchello, B., Wang, M., Fethi, A., 2018. Process analysis and economic evaluation of mixed aqueous ionic liquid and monoethanolamine (MEA) solvent for CO2 capture from a coke oven plant. Greenh. Gases: Sci. Technol. 8, 686–700. https://doi.org/10.1002/ghg.1772.
Onarheim, K., Arasto, A., 2016. Staged implementation of alternative processes in an existing integrated steel mill for improved performance and reduced CO2 emissions – Part I: technical concept analysis. Int. J. Greenh. Gas Control 45, 163–171. https://doi.org/10.1016/j.ijggc.2015.12.008.
Perpiñán, J., Peña, B., Bailera, M., Eveloy, V., Kannan, P., Raj, A., Lisbona, P., Romeo, L. M., 2023. Integration of carbon capture technologies in blast furnace based steel making: A comprehensive and systematic review. Fuel 336, 127074. https://doi.org/10.1016/j.fuel.2022.127074.
Petrescu, L., Chisalita, D.-A., Cormos, C.-C., Manzolini, G., Cobden, P., van Dijk, H.A.J., 2019. Life cycle assessment of SEWGS technology applied to integrated steel plants. Sustainability 11. https://doi.org/10.3390/su11071825.
Qie, Y., Lyu, Q., Lan, C., Zhang, S., 2020. Energy conservation and CO2 abatement potential of a gas-injection blast furnace. High Temp. Mater. Process. 39, 96–106. https://doi.org/10.1515/htmp-2020-0031.
Quader, M.A., Ahmed, Shamsuddin, Raja Ghazilla, R.A., Ahmed, Shameem, Dahari, M., 2016. Evaluation of criteria for CO2 capture and storage in the iron and steel industry using the 2-tuple DEMATEL technique. J. Clean. Prod 120, 207–220. https://doi.org/10.1016/j.jclepro.2015.10.056.
Ramírez-Santos, Á.A., Bozorg, M., Addis, B., Piccialli, V., Castel, C., Favre, E., 2018. Optimization of multistage membrane gas separation processes. Example of application to CO2 capture from blast furnace gas. J Memb Sci 566, 346–366. https://doi.org/10.1016/j.memsci.2018.08.024.
Remus, R., Aguado-Monsonet, M.A., Roudier, S., Delgado Sancho, L., 2013. Best available techniques (BAT) reference document for Iron and Steel production - Industrial Emissions Directive 2010/75/EU (Integrated Pollution Prevention and Control).
Sahu, R.K., Roy, S.K., Sen, P.K., 2015. Applicability of top gas recycle blast furnace with downstream integration and sequestration in an integrated steel plant. Steel. Res. Int 86, 502–516. https://doi.org/10.1002/srin.201400196.
She, X., An, X., Wang, J., Xue, Q., Kong, L., 2017. Numerical analysis of carbon saving potential in a top gas recycling oxygen blast furnace. J. Iron Steel Res. Int. 24, 608–616. https://doi.org/10.1016/S1006-706X(17)30092-4.
Smith, E., Morris, J., Kheshgi, H., Teletzke, G., Herzog, H., Paltsev, S., 2021. The cost of CO2 transport and storage in global integrated assessment modeling. Int. J. Greenh. Gas Control 109, 103367. https://doi.org/10.1016/j.ijggc.2021.103367.
Ströhle, J., Junk, M., Kremer, J., Galloy, A., Epple, B., 2014. Carbonate looping experiments in a 1 MWth pilot plant and model validation. Fuel 127, 13–22. https://doi.org/10.1016/j.fuel.2013.12.043.
Sun, Zhao, Liu, J., Sun, Zhiqiang, 2020. Synergistic decarbonization and desulfurization of blast furnace gas via a novel magnesium-molybdenum looping process. Fuel 279, 118418. https://doi.org/10.1016/j.fuel.2020.118418.
Sundqvist, M., Biermann, M., Normann, F., Larsson, M., Nilsson, L., 2018. Evaluation of low and high level integration options for carbon capture at an integrated iron and steel mill. Int. J. Greenh. Gas Control 77, 27–36. https://doi.org/10.1016/j.ijggc.2018.07.008.
Tian, S., Jiang, J., Zhang, Z., Manovic, V., 2018. Inherent potential of steelmaking to contribute to decarbonisation targets via industrial carbon capture and storage. Nat. Commun 9, 4422. https://doi.org/10.1038/s41467-018-06886-8.
Tsupari, E., Kärki, J., Arasto, A., Lilja, J., Kinnunen, K., Sihvonen, M., 2015. Oxygen blast furnace with CO2 capture and storage at an integrated steel mill – Part II: economic

feasibility in comparison with conventional blast furnace highlighting sensitivities. Int. J. Greenh. Gas Control 32, 189–196. https://doi.org/10.1016/j.ijggc.2014.11.007.

Tsupari, E., Kärki, J., Arasto, A., Pisilä, E., 2013. Post-combustion capture of CO2 at an integrated steel mill - part II: economic feasibility. Int. J. Greenh. Gas Control 16, 278–286. https://doi.org/10.1016/j.ijggc.2012.08.017.

van Dijk, H.A.J., Cobden, P.D., Lukashuk, L., de Water, L.van, Lundqvist, M., Manzolini, G., Cormos, C.-C., van Dijk, C., Mancuso, L., Johns, J., Bellqvist, D., 2018. STEPWISE Project: sorption-enhanced water-gas shift technology to reduce carbon footprint in the iron and steel industry. Johns. Matthey Technol. Rev. 62, 395–402. https://doi.org/10.1595/205651318X15268923666410.

Wiley, D.E., Ho, M.T., Bustamante, A., 2011. Assessment of opportunities for CO2 capture at iron and steel mills: an Australian perspective. Energy Procedia 4, 2654–2661. https://doi.org/10.1016/j.egypro.2011.02.165.

Wright, A.D., White, V., Hufton, J.R., Quinn, R., Cobden, P.D., van Selow, E.R., 2011. CAESAR: development of a SEWGS model for IGCC. Energy Procedia 4, 1147–1154. https://doi.org/10.1016/j.egypro.2011.01.167.

Xiang, D., Zhao, S., 2018. Parameter optimization and thermodynamic analysis of COG direct chemical looping hydrogen processes. Energy Convers. Manage 172, 1–8. https://doi.org/10.1016/j.enconman.2018.07.007.

Xie, H., Yu, Q., Zhang, Y., Zhang, J., Liu, J., Qin, Q., 2017. New process for hydrogen production from raw coke oven gas via sorption-enhanced steam reforming: thermodynamic analysis. Int. J. Hydrog. Energy 42, 2914–2923. https://doi.org/10.1016/j.ijhydene.2016.12.046.

Yan, Y., Manovic, V., Anthony, E.J., Clough, P.T., 2020. Techno-economic analysis of low-carbon hydrogen production by sorption enhanced steam methane reforming (SE-SMR) processes. Energy Convers. Manage 226. https://doi.org/10.1016/j.enconman.2020.113530.

Yun, S., Jang, M.-G., Kim, J.-K., 2021. Techno-economic assessment and comparison of absorption and membrane CO2 capture processes for iron and steel industry. Energy 229, 120778. https://doi.org/10.1016/j.energy.2021.120778.

Zecca, N., Cobden, P.D., Lücking, L., Manzolini, G., 2023. SEWGS integration in a direct reduction steelmaking process for CO2 mitigation. Int. J. Greenh. Gas Control 130. https://doi.org/10.1016/j.ijggc.2023.103991.

Zecca, N., Lücking, L., Chisăliță, D.-A., Boon, J., van Dijk, H.A.J., Pieterse, J.A.Z., Giuffrida, A., Manzolini, G., 2025. DISPLACE post-combustion carbon capture technology integration in a steel plant for CO2 reduction. J. Clean. Prod, 144739. https://doi.org/10.1016/j.jclepro.2025.144739.

Zuo, Guangqing, Hirsch, A., 2009. The trial of the top gas recycling blast furnace at LKAB's EBF and scale-up. Rev. Met. Paris 106, 387–392. https://doi.org/10.1051/metal/2009067.